MCTP-08-64

Non-minimal universal extra dimensions

Thomas Flacke[a], A. Menon[a], and Daniel J. Phalen[a]

[a] *Michigan Center for Theoretical Physics (MCTP)*
Randall Laboratory, Physics Department, University of Michigan
Ann Arbor, MI 48109

(Dated: March 19, 2009)

Abstract

In this paper we investigate the phenomenological implications of boundary localized terms (BLTs) in the model of Universal Extra Dimensions (UED). In particular, we study the electroweak Kaluza-Klein mass spectrum resulting from BLTs and their effect on electroweak symmetry breaking via the five dimensional Higgs mechanism. We find that the addition of BLTs to massive five dimensional fields induces a non-trivial extra dimensional profile for the zero and non-zero Kaluza-Klein (KK) modes. Hence BLTs generically lead to a modification of Standard Model parameters and are therefore experimentally constrained, even at tree level. We study Standard Model constraints on three representative non-minimal UED models in detail and find that the constraints on BLTs are weak. On the contrary, non-zero BLTs have a major impact on the spectrum and couplings of non-zero KK modes. For example, there are regions of parameter space where the Lightest Kaluza-Klein particle (LKP) is either the Kaluza-Klein Higgs boson or the first KK mode of the W^3.

1 Introduction

In models with an Universal Extra Dimension (UED) [1], all Standard Model particles are promoted to 5 dimensional fields propagating in a flat extra dimension.[1] The extra dimension is chosen to be the orbifold $S^1/\mathbb{Z}_2$, and with the appropriate boundary conditions one can obtain chiral fermions and avoid the massless scalar modes associated with the zero modes of the extra gauge field components. Due to the $\mathbb{Z}_2$ symmetry, the interactions between the Kaluza-Klein (KK) modes respect a $\mathbb{Z}_2$ parity called KK parity. KK parity implies that Kaluza Klein particles can only be produced pairwise, leading to a lower bound on the KK mass scale (M_{kk}) of about 500 GeV, which can be probed by the Large Hadron Collider. Furthermore, KK parity guarantees the stability of the lightest Kaluza-Klein particle (LKP), thus providing UED with a dark matter candidate.

At tree-level, UED is a simple extension of the Standard Model with only two experimentally undetermined parameters: the compactification radius R and the Higgs mass $m_{\rm h}$. However, since UED is a 5 dimensional theory, it is non-renormalizable and therefore should be considered to be an effective field theory. The cutoff for UED can be estimated by naive dimensional analysis to be $\Lambda \sim 50 M_{kk}$ [3], where the Kaluza-Klein mass scale $M_{kk} \equiv 1/R$ is set by the compactification radius R.[2] Treating UED as an effective field theory implies that all operators that are allowed by the Standard Model gauge symmetries and 4 dimensional Lorentz invariance should be included in the theory. Such operators can be in the bulk or localized at the orbifold fixed points so there are many more undetermined tree level parameters than (R, m_h).

To our knowledge, all phenomenological UED studies of bounds from colliders [5], electroweak precision [6], flavor changing neutral currents [7, 8] and other precision measurements [9] have focused on either the tree level couplings and mass spectrum of UED without boundary localized terms (which we will refer to as "standard" UED) or on the one loop modified mass spectrum and couplings of Minimal UED (MUED) [10]. In the MUED scenario, all boundary localized terms are assumed to be zero at the cutoff scale Λ and are induced at low scales due to renormalization group evolution. Studies of UED dark matter [11, 12, 13, 14] often make less strong assumptions about the details of the KK mass spectrum, but assume that the couplings of the first KK level excitations are identical to those of the Standard model. A further important task is to distinguish UED from other Standard Model extensions [15]. If beyond the Standard Model signals are found at the LHC, they should be studied in the full UED parameter space.[3]

In this article, we study the phenomenological impact of including boundary localized terms (BLTs) for the electroweak sector of UED. The electroweak sector is of interest because it hosts many of the phenomenologically viable dark matter candidates: the first KK mode of the B gauge boson $B^{(1)}$, the first KK mode of the neutral component of the W gauge boson $W^{3(1)}$, the first KK mode of the Higgs boson $h^{(1)}$ and the electrically

[1] For pre-dating ideas closely related to UED models see Refs. [2].

[2] Studies of unitarity bounds on heavy gluon scattering also impose bounds on the number of KK states included in the effective 4D theory, typically implying $\Lambda < \mathcal{O}(10) M_{kk}$ [4].

[3] For a detailed review on the current status of UED, see Ref. [16].

neutral pseudoscalar Higgs boson $a^{0(1)}$.[4] The BLTs we consider are boundary localized kinetic terms for the B and W gauge bosons and boundary localized kinetic, mass, and quartic terms for the Higgs boson. Of the possible additional effective operators that are compatible with 4 dimensional Lorentz invariance and the Standard Model gauge symmetries, these BLTs have the lowest mass dimension. We find that the zero mode wavefunctions of the massive 5 dimensional fields with BLTs are not generally flat, which in UED generically leads to modified zero mode couplings. As the zero modes of the 5 dimensional fields are to be identified with the Standard Model, these modifications translate into constraints on the size of these boundary localized operators. We find these constraints are weak, leaving regions of allowed parameter space where the LKP is the KK Higgs $h^{(1)}$ and other, extended regions in which the LKP is $W^{3(1)}$-like. We would like to emphasize that our analysis is complementary to that of MUED in Ref. [10] because we assume that the effects of BLTs dominate those induced by loop effects and our analysis is purely at tree level.

The article is organized as follows: in Section 2 we provide a brief review of the "standard" UED model. We concentrate on the structure of the KK decomposition and the basic relations between the 4 dimensional and 5 dimensional masses and couplings in order to compare them to the modified relations established in the latter part of the paper. To include BLTs in UED we need to KK expand the extra dimensional fields in the presence of BLTs and extend the standard UED gauge fixing procedure of Ref. [17] to identify the physical Higgs and Goldstone modes at each KK level.

In Section 3 we consider the toy model of a massive 5 dimensional scalar field on $S_1/\mathbb{Z}_2$ with boundary localized kinetic terms (BLKTs) and boundary localized mass terms (BMTs) to demonstrate the effect of BLTs on the wavefunctions of an extra dimensional field. We find that the mass spectrum and wavefunctions are significantly modified by BLTs. In particular, the wavefunction of the zero mode becomes non-flat. The transcendental equations that determine the scalar KK mode masses in Ref. [18] are modified due to the additional 5 dimensional bulk mass parameter. These KK mode mass relations, wavefunctions and normalizations remain the same for gauge fields and hence can be translated directly into those for the electroweak sector. A generalization of the UED gauge fixing procedure necessary for the identification of the boundary conditions of the physical Higgses $a^{\pm}$ and a^0 is worked out in the Appendices A and B. In particular we determine the Goldstone's, pseudoscalar's, and charged Higgs bosons' equations of motion and their boundary conditions in unitary gauge. From their boundary conditions we are able to determine the mass spectrum of the pseudoscalars and their couplings.

In Section 4 we use these results to present the KK decomposition of the complete electroweak sector in UED and the modifications of couplings of the KK modes as well as the zero modes. Using these mass relations and couplings we discuss the phenomenological consequences of the BLTs in Section 5. We study three sample scenarios in detail in order to illustrate the constraints and novel phenomenology of non-minimal UED. In

[4]The KK neutrino $\nu^{(1)}$ is experimentally disfavored, if standard UED couplings are assumed. Direct detection limits on a KK neutrino scattering off a nucleon through a t-channel Z boson puts a bound of $M_\nu^{(1)} \gtrsim 50\,\text{TeV}$ [11], while requiring that the KK neutrino does not over close the universe requires $M_\nu^{(1)} \lesssim 3\,\text{TeV}$ [12].

scenario I, we assume uniform electroweak BLKTs and vanishing Higgs boundary mass and quartic terms, while in scenario II we allow the Higgs BLKT to differ from the uniform gauge BLKT, and in scenario III we allow the $U(1)_Y$ and $SU(2)$ BLKTs to differ. For each of these scenarios we match the tree-level zero mode masses and spectra to that of the Standard Model to constrain the size of the BLTs. For scenario I, the LKP is the KK photon, while for scenario II there are regions of allowed parameter space with a Higgs LKP. For scenario III, the LKP is the W^3 in most of the parameter space. Finally in Section 6 we conclude.

2 UED mass spectrum and couplings: a mini review

In this section we briefly review the theoretical setup of universal extra dimensions (UED) and discuss its mass spectrum and couplings in the absence of large BLTs.[5]

2.1 UED at tree level

The UED bulk action on $S^1/\mathbb{Z}_2$ is

$$S_{UED,bulk} = S_g + S_H + S_f \tag{1}$$

with

$$\begin{aligned} S_g &= \int d^5x \left(-\frac{1}{4\hat{g}_3^2} G^A_{MN} G^{AMN} - \frac{1}{4\hat{g}_2^2} W^I_{MN} W^{IMN} - \frac{1}{4\hat{g}_Y^2} B_{MN} B^{MN} \right) && (2) \\ S_H &= \int d^5x \left((D_M H)^\dagger (D^M H) + \hat{\mu}^2 H^\dagger H - \hat{\lambda} (H^\dagger H)^2 \right) && (3) \\ S_f &= \int d^5x \left(i\overline{f}\gamma^M D_M f + \left(\hat{\lambda}_E \overline{L} E H + \hat{\lambda}_U \overline{Q} U \tilde{H} + \hat{\lambda}_D \overline{Q} D H + \text{h.c.} \right) \right) && (4) \end{aligned}$$

where $x_5 \equiv y \in [0, \pi R]$, G_{MN}, W_{MN}, B_{MN} are the 5 dimensional $SU(3)_C \times SU(2)_W \times U(1)_Y$ gauge field strengths, $f = (Q, U, D, L, E)$ denote the 5 dimensional fermion fields, D_M is the corresponding 5 dimensional covariant derivative and the hatted quantities denote the 5 dimensional couplings.

In order to obtain the Standard Model spectrum at the zero mode level, Neumann boundary conditions are imposed on the $H, G^A_\mu, W^I_\mu, B_\mu, Q_L, L_L, U_R, D_R, E_R$ fields while Dirichlet boundary conditions are imposed on the $G^A_5, W^I_5, B_5, Q_R, L_R, U_L, D_L, E_L$ fields. If no boundary terms are present, all bulk fields can be decomposed in terms of the *same* KK mode basis $\{f^{(n)}\} \propto \{\sin(ny/\pi R), \cos(ny/\pi R)\}$.[6] Integration over the extra dimension yields the effective 4 dimensional action in terms of the Standard Model and its KK partners. Matching the zero mode masses and couplings to the Standard Model fixes all 5 dimensional parameters in terms of the Standard Model observables

[5] See Refs. [1, 16].

[6] For details on the fermion decomposition see Ref. [7].

multiplied by the appropriate factors of πR.. The only free parameters at tree level are the compactification radius R and the Higgs mass m_h.

At the non-zero KK levels, the spectrum contains a partner for every Standard Model particle with a mass $m_{\Phi^{(n)}} = \sqrt{(n/R)^2 + m^2_{\Phi^{(0)}}}$, where $m^2_{\Phi^{(0)}}$ is the corresponding zero mode mass. In addition to these fields, at each non-zero KK level a charged Higgs $a^{\pm}$ and a pseudoscalar Higgs a^0 are also present. The extra Higgs bosons are present because at the n$^{\text{th}}$ KK level there are eight scalar degrees of freedom due to the $W_5^{I(n)}$, $B_5^{(n)}$ and the Higgs boson $H^{(n)}$. A linear combination of four of these scalars form the longitudinal components of the $B_\mu^{(n)}$ and $W_\mu^{a(n)}$ gauge bosons. The remaining four degrees of freedom form the KK Higgs boson $h^{(n)}$, the charged Higgs $a^{\pm(n)}$ and the pseudoscalar Higgs $a^{0(n)}$ with masses $m_{h^{(n)}} = \sqrt{(n/R)^2 + m^2_{h^{(0)}}}$, $m_{a^{\pm(n)}} = m_{W^{\pm(n)}}$, and $m_{a^{0(n)}} = m_{Z^{(n)}}$. Hence the particle spectrum at any non-zero KK mode is almost degenerate. A detailed discussion of the electroweak sector including the identification of the Goldstone and the physical Higgs mode and their KK decomposition can be found in Ref. [17]. It is important to note that in the electroweak sector, mixing occurs between $B_\mu^{(n)}$ and $W_\mu^{(n)}$ as well as in the Goldstone - Higgs sector. In the absence of BLTs, the KK bases of all fields are identical and therefore orthogonality guarantees no mixing between different KK-levels. All non-zero tree-level couplings of the heavier KK modes are the same as those of the zero mode as long as the vertex satisfies KK number conservation. KK number is violated at loop level but $\mathbb{Z}_2$ symmetry guarantees the stability of the lightest KK particle.

2.2 UED as an effective field theory

As a five dimensional quantum field theory, UED is non-renormalizable and should be considered to be an effective field theory. Naive dimensional analysis suggests that a perturbative description of UED is valid up to the energy scale $\Lambda \sim 50/R$ [3]. Studies of unitarity bounds on heavy gluon scattering also impose bounds on the number of KK states included in the effective 4D theory, typically implying $\Lambda < \mathcal{O}(10) M_{KK}$ [4]. Hence for a phenomenologically interesting compactification radius of $R^{-1} \sim 1$ TeV, the cutoff of the theory is relatively low. Without a better understanding of the high scale completion of UED we cannot *a priori* neglect allowed operators, but we should instead try to use experimental data to put constraints on the size of these operators. The set of operators that agree with 4 dimensional Lorentz invariance, $\mathbb{Z}_2$ parity, and the gauge symmetries of the Standard Model include higher dimensional operators in the bulk and boundary localized operators at the fixed points of the $S^1/\mathbb{Z}_2$ compactified extra dimension.

Boundary localized operators contain the lowest dimensional operators beyond the "standard" UED operators and therefore should be included in any realistic phenomenological treatment of UED. Furthermore, even if the BLTs are set to zero at tree-level, they will be generated at the one-loop level [10, 19]. In particular, *every* bulk term in the action in Eq. (1) can be accompanied by a corresponding boundary localized operator at each orbifold fixed point, and the size of these boundary localized operators needs to be equal due to $\mathbb{Z}_2$ symmetry. The most studied effective field theoretic description of

UED is "Minimal" UED [10]. In MUED there are three undetermined parameters: the compactification scale R^{-1}, the Higgs mass m_h and the cutoff scale Λ. All the BLTs are assumed to vanish at the cutoff scale Λ but are induced by RG running from Λ down to the electroweak scale. The RG evolution of the bulk and boundary terms induces significant changes in the particle spectrum and lifts some of the degeneracies of tree-level UED. One of the most striking features of the one-loop corrected mass spectrum is that the Weinberg angle differs for different KK levels. The LKP, being the lighter eigenstate of the $B^{(1)} - W^{3(1)}$ system, turns out to be almost purely $B^{(1)}$.

In this paper we assume large BLTs at the electroweak scale and study the impact of including these terms on tree-level Standard Model observables. This setup is non-minimal because we relax the assumption of vanishing BLTs at the cutoff scale.

3 Boundary localized terms for massive bulk fields

When compactifying a higher dimensional field on a flat manifold, the KK modes can be understood as discrete eigenstates of momentum in the extra dimension. KK number conservation in interactions is a remnant of five dimensional momentum conservation. BLTs violate 5 dimensional translational invariance and therefore induce mixing between the modes of well defined KK number. If the BLTs are sufficiently suppressed they can be treated as perturbations and dealt with as mass insertions. Since we want to allow for large BLTs, the mass insertions due to BLTs can no longer be treated perturbatively.

The problem of boundary localized kinetic terms (BLKTs) in 5 dimensional theories has been addressed in Refs. [18, 20, 21]. In Ref. [18], it was shown that a 5 dimensional massless scalar field Φ with a localized brane kinetic term at $y = 0$ of the form

$$S_{BLKT} = \frac{r_\Phi}{2} \int d^5x \; \partial_\mu \Phi \partial^\mu \Phi \delta(y), \tag{5}$$

can be decomposed into KK modes by demanding that its wavefunctions f_n satisfy the modified orthogonality relations

$$\begin{aligned} \int dy \left[1 + r_\Phi \delta(y)\right] f_n(y) f_m(y) &= \delta_{nm} \\ \int dy (\partial_5 f_n(y))(\partial_5 f_m(y)) &= m^2_{\Phi^{(n)}} \delta_{nm}, \end{aligned} \tag{6}$$

where $m_{\Phi^{(n)}}$ is the n^{th} KK mode mass. Ref. [20] showed that the same prescription works for massless gauge fields. The inclusion of a second brane at πR due to the $\mathbb{Z}_2$ symmetry just changes $\delta(y)$ to $[\delta(y) + \delta(y - \pi R)]$ in Eq. (6). Including BLKTs reduces the non-zero KK mode masses to values below those of "standard" UED. The zero mode is still massless and zero mode wavefunctions are still flat.

Using these results we can now consider the case of a massive 5 dimensional scalar which has both boundary localized mass terms and boundary localized kinetic terms. The bulk action on $S^1/\mathbb{Z}_2$ is

$$S = \frac{1}{2} \int d^5x \left(\partial^M \Phi \partial_M \Phi - m^2 \Phi^2 \right), \tag{7}$$

which leads to the equation of motion

$$(\Box - \partial_5^2 + m^2)\Phi = 0. \tag{8}$$

Using separation of variables we decompose the 5 dimensional scalar into the form

$$\Phi(x,y) \;=\; \sum_i \Phi^{(i)}(x) f_i(y), \tag{9}$$

so that the equations of motion are

$$\begin{aligned} \Box\Phi(x) &= -m_i^2 \Phi^{(i)}(x) && (10)\\ f_i''(y) &= -(m_i^2 - m^2) f_i(y) \equiv -M_i^2 f_i(y). && (11) \end{aligned}$$

Due to $S^1/\mathbb{Z}_2$ symmetry, the solutions to Eq. (11) are odd or even under $\mathbb{Z}_2$ and are given by

$$f_\alpha = N_\alpha \begin{cases} \frac{\cosh\left(M_\alpha\left(y-\frac{\pi R}{2}\right)\right)}{\cosh\left(\frac{M_\alpha \pi R}{2}\right)} & \alpha \text{ even} \\ -\frac{\sinh\left(M_\alpha\left(y-\frac{\pi R}{2}\right)\right)}{\sinh\left(\frac{M_\alpha \pi R}{2}\right)} & \alpha \text{ odd} \end{cases} \tag{12}$$

$$f_n = N_n \begin{cases} \frac{\cos\left(M_n\left(y-\frac{\pi R}{2}\right)\right)}{\cos\left(\frac{M_n \pi R}{2}\right)} & n \text{ even} \\ -\frac{\sin\left(M_n\left(y-\frac{\pi R}{2}\right)\right)}{\sin\left(\frac{M_n \pi R}{2}\right)} & n \text{ odd} \end{cases}, \tag{13}$$

where the physical masses are

$$\begin{aligned} m_\alpha^2 &= -M_\alpha^2 + m^2 \\ m_n^2 &= M_n^2 + m^2, && (14) \end{aligned}$$

and we use lower case Greek indices for the hyperbolic solutions and lower case Latin indices for the trigonometric solutions.[7]

So far, our discussion has been independent of the BLTs, which enter in two ways. First, BLTs modify the normalization conditions that determine the coefficients N_α and N_n. Second, they modify the variation of the action on the boundary. In order to find a consistent solution, the bulk *and* the boundary variations of the action must vanish. The boundary variation has contributions from the bulk via partial integrations in y and directly from the variation of BLTs. Requiring that the boundary variation vanish leads to boundary conditions on Φ, which result in a quantization condition on M_i.

Adding the following BLTs

$$S_{bd} = \frac{1}{2}\int d^5x \left(r_\Phi \partial^\mu \Phi \partial_\mu \Phi - m_b^2 \Phi^2\right)\left[\delta(y) + \delta(y-\pi R)\right], \tag{15}$$

[7]Depending on the choice of boundary terms, the hyperbolic equation has zero, one or two solutions. For the case of a hyperbolic solution the physical mass m_α^2 always remains positive.

we find the modified boundary conditions

$$0 = [\partial_5 - (r_\Phi \Box + m_b^2)]\Phi|_{y=0} \quad (16)$$
$$0 = [\partial_5 + (r_\Phi \Box + m_b^2)]\Phi|_{y=\pi R}, \quad (17)$$

where r_Φ is the brane kinetic parameter and m_b is the brane mass term. If we use the wavefunctions in Eq. (12) and Eq. (13) we find the "hyperbolic" quantization conditions

$$b_\alpha \equiv \frac{(r_\Phi m_\alpha^2 - m_b^2)}{M_\alpha} = \begin{cases} \tanh(\frac{M_\alpha \pi R}{2}) & \text{even} \\ \coth(\frac{M_\alpha \pi R}{2}) & \text{odd} \end{cases} \quad (18)$$

and the "trigonometric" quantization conditions

$$b_n \equiv \frac{(r_\Phi m_n^2 - m_b^2)}{M_n} = \begin{cases} -\tan(\frac{M_n \pi R}{2}) & n \text{ even} \\ \cot(\frac{M_n \pi R}{2}) & n \text{ odd.} \end{cases} \quad (19)$$

The wavefunctions $\{f_n\}$, $\{f_\alpha\}$ in Eq. (12) and Eq. (13) are pairwise orthonormal with respect to the modified scalar product

$$\int_0^{\pi R} dy \left[1 + r_\Phi \left[\delta(y) + \delta(y - \pi R)\right]\right] f_i f_j = \delta_{ij}, \quad (20)$$

resulting in the normalizations

$$N_\alpha^{-2} = \begin{cases} \text{sech}^2\left(\frac{M_\alpha \pi R}{2}\right)\left[\frac{\sinh(M_\alpha \pi R)}{2M_\alpha} + \frac{\pi R}{2}\right] + 2r_\Phi & \text{even} \\ \text{cosech}^2\left(\frac{M_\alpha \pi R}{2}\right)\left[\frac{\sinh(M_\alpha \pi R)}{2M_\alpha} - \frac{\pi R}{2}\right] + 2r_\Phi & \text{odd} \end{cases} \quad (21)$$

$$N_n^{-2} = \begin{cases} \sec^2\left(\frac{M_n \pi R}{2}\right)\left[\frac{\pi R}{2} + \frac{\sin(M_n \pi R)}{2M_n}\right] + 2r_\phi & \text{even} \\ \text{cosec}^2\left(\frac{M_n \pi R}{2}\right)\left[\frac{\pi R}{2} - \frac{\sin(M_n \pi R)}{2M_n}\right] + 2r_\phi & \text{odd} \end{cases} . \quad (22)$$

Eq. (18) and Eq. (19) show the dependence of the KK masses on the brane kinetic parameter r_Φ and the brane mass term m_b. If $r_\Phi m^2 < m_b^2$, there is no hyperbolic solution, while for $r_\Phi m^2 > m_b^2$ one or two hyperbolic solutions are possible. In addition, a flat zero mode wavefunction is only possible when

$$r_\Phi m^2 = m_b^2. \quad (23)$$

The physical masses for these solutions interpolate smoothly for different values of r_Φ, m_b, m and R^{-1}.

In Fig. 1 we show the variation of the mass spectrum for different values of r_Φ and m_b. Boundary localized kinetic terms have the effect of decreasing the n^{th} KK mass below that of $\sqrt{(n/R)^2 + m^2}$ while boundary localized mass terms have the opposite effect of increasing KK masses. In the limit $r_\Phi/R \to \infty$, the second KK mode mass, m_2, is bounded from below by $\sqrt{(1/R)^2 + m^2}$, while zero and first KK modes become massless. Thus, when identifying the zero mode with a Standard Model particle, the mass splitting between the first and second KK mode can be made arbitrarily large.

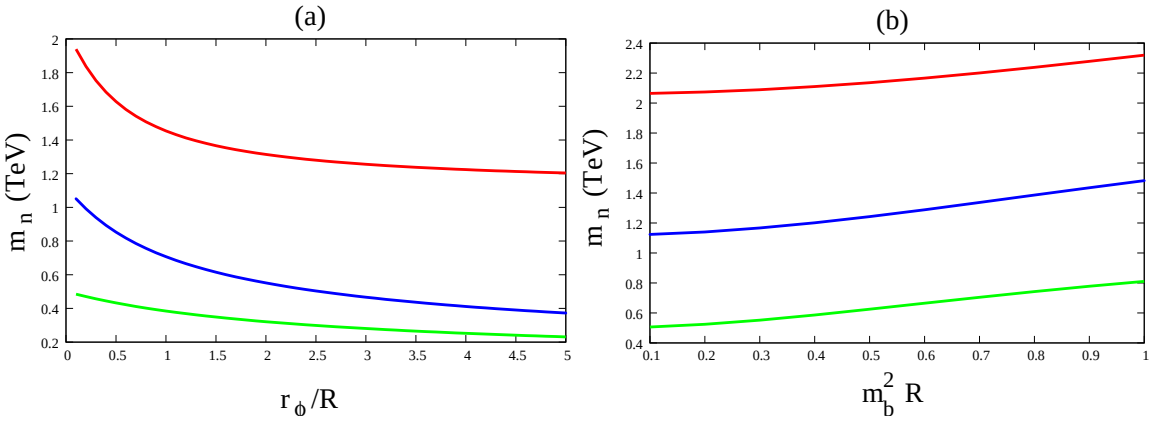

Figure 1: (a) Variation of the KK spectrum as a function r_Φ with $R^{-1} = 1$ TeV, $m = .5$ TeV $m_b = 0$. (b) Variation of the KK spectrum for as a function of m_b with $R^{-1} = 1$ TeV, $m = .5$ TeV $r_\Phi = 0$. The green (light gray) curve corresponds to the variation of the zero mode mass, the blue (black) curve corresponds to the variation of the first KK mode mass, and the red (dark gray) corresponds to the variation of the second KK mode mass.

4 UED with boundary localized terms

In this section we apply the results of the scalar toy model to the full UED spectrum. We include only electroweak BLTs because many potentially viable dark matter candidates are present in the first KK level of the electroweak sector. Hence the BLTs we consider are

$$\begin{aligned} S_{BLT} &= \int d^5x \left[\delta(y) + \delta(y - \pi R)\right] \times \\ &\quad \Big(-\frac{r_B}{4\hat{g}_Y^2} B_{\mu\nu} B^{\mu\nu} - \frac{r_W}{4\hat{g}_2^2} W^a_{\mu\nu} W^{a\mu\nu} \\ &\quad + r_H (D^\mu H)^\dagger D_\mu H + \mu_b^2 H^\dagger H - \lambda_b (H^\dagger H)^2 \Big) \end{aligned} \tag{24}$$

where r_B, r_W, r_H are constants, which from naive dimensional analysis have a natural value of the order of $\frac{6\pi}{\Lambda}$, where Λ is the cutoff scale [20].

The BLTs in Eq. (24) respect the $SU(2) \times U(1)_Y$ gauge symmetry and Lorentz invariance on the brane. Their presence breaks 5 dimensional translation invariance, which, however, is already broken by the presence of the branes. We will work in the limit of zero brane thickness, so that brane terms containing ∂_5 do not affect the KK spectrum [20, 21] and therefore the kinetic terms we consider are parallel to the brane. For the boundary Higgs potential we assume the fine tuned condition $\hat{v} \equiv \sqrt{\hat{\mu}^2/\hat{\lambda}} = \sqrt{\mu_b^2/\lambda_b}$, which guarantees, that the expansion of the Higgs around the VEV $\hat{v}(y) = \hat{v} = const$ is consistent with the bulk and boundary variations.[8]

[8]For studies of electroweak symmetry breaking in the presence of a non-constant VEV but in absence of boundary kinetic terms see Refs [22].

Following the spirit of the last section, we need to find the bulk equations of motion for all fields in the electroweak sector and then determine the KK decomposition from their boundary conditions. The boundary conditions include terms from the variation of the bulk action on the boundary as well as BLTs. For the electroweak sector of UED, the situation is complicated by the mixing between the B_μ and W^3_μ gauge bosons, as well as the mixing between the B_5, W^3_5, and the Higgs field which contain the Goldstone and the physical Higgs modes. In order to identify the physical Higgs modes and the correct boundary conditions for the Higgs and gauge fields, we reformulate the KK decomposition procedure of Ref. [17] along the lines of Ref. [23] in Appendices A and B. The manifestly 5 dimensional formulation of the Goldstone bosons and Higgs fields enables us to incorporate the BLTs of Eq. (24) and determine the boundary conditions.

In the following subsections, we present the bulk equations of motion (which are unmodified by the boundary terms), their boundary conditions as derived in Appendices A and B, and discuss the mass spectrum and couplings of all zero and KK modes in the electroweak sector. For convenience, the results are summarized in Appendix C.

4.1 The Higgs mass spectrum and wavefunctions

For the Higgs, the bulk equations of motion and boundary conditions are given by

$$\left[\Box - \partial_5^2 + 2\hat{\mu}^2\right] h = 0 \tag{25}$$

$$\left[\pm\partial_5 + (r_H \Box + 2\mu_b^2)\right] h|_{y=\pi R,0} = 0, \tag{26}$$

where the $+\partial_5$ ($-\partial_5$) corresponds to the boundary condition at πR (0), which is similar to those of massive scalar in Section 3. Hence we can determine the mass quantization conditions, wavefunctions and normalization factors from the corresponding results of Section 3 using the identifications: $r_\Phi \to r_H$, $m^2_\Phi \to 2\hat{\mu}^2$, and $m^2_b \to 2\mu^2_b$.

The Higgs KK masses can be lowered by increasing r_H and raised by increasing μ_b. As the Standard Model Higgs has not been found, the only phenomenological bound on $\hat{\mu}$ and μ_b is, that the zero mode mass must be greater than 115 GeV. However in the next section we will see that r_H is constrained because it influences the gauge boson masses.

4.2 Mass spectrum of the charged electroweak sector

The charged gauge bosons are decomposed so that their equations of motion and boundary conditions are[9]

$$\left[\left(\Box - \partial_5^2 + \frac{\hat{g}_2^2 \hat{v}^2}{4}\right)\eta^{\mu\nu} - \partial^\mu\partial^\nu\right] W^\pm_\mu = 0 \tag{27}$$

$$\left(\pm\partial_5 + r_W\left[\Box\eta^{\mu\nu} - \partial^\mu\partial^\nu\right] + r_H\left(\frac{\hat{g}_2\hat{v}}{2}\right)^2\right) W^\pm_\nu|_{y=\pi R,0} = 0 \tag{28}$$

[9]The details of gauge fixing in the presence of boundary terms is discussed in Appendices A and B. The results we quote here are in unitary gauge.

which resembles those of the scalar model in Section 3. Again, the mass determining equations and wavefunctions can be read off from Section 3 using the identifications $r_\Phi \to r_W$, $m_\Phi^2 \to \hat{g}_2^2\hat{v}^2/4$, and $m_b^2 \to r_H\hat{g}_2^2\hat{v}^2/4$. For the normalization conditions, we rescale Eq. (20) by $\hat{g}_2^2$ so that

$$\frac{1}{\hat{g}_2^2}\int_0^{\pi R} dy\,[1 + r_W\,[\delta(y) + \delta(y-\pi R)]]\,f_i^W f_j^W = \delta_{ij}, \tag{29}$$

which guarantees the canonical normalization of kinetic terms for each KK mode. The boundary "mass" term for the W boson is induced by the boundary interaction term $\mathcal{L}_{BLT} \supset \frac{r_H}{4}H^\dagger H W_\mu^+ W^{-\mu}$ in Eq. (24) when electroweak symmetry breaking occurs. Note that the condition for a flat zero mode in Eq. (23) translates into $r_W = r_H$. Unless the Higgs and gauge BLKT parameters are identical, $W^{\pm(0)}$ has a y-dependent profile.

Apart from the charged gauge bosons, as explained in Section 2, UED also contains charged Higgses at non-zero KK levels. According to Appendices A and B, the equation of motion and boundary conditions of the charged Higgs boson are

$$\left(\Box - \partial_5^2 + \frac{\hat{g}_2^2\hat{v}^2}{4}\right)a^\pm = 0 \tag{30}$$

$$(a^\pm \pm r_H\partial_5 a^\pm)|_{y=\pi R,0} = 0. \tag{31}$$

Using the results of Section 3 along with the identification $r_\Phi \to r_H$, $m_\Phi^2 \to \hat{g}_2^2\hat{v}^2/4$, and $m_b^2 \to r_H\hat{g}_2^2\hat{v}^2/4$, we can find the $a^\pm$ mass determining equations and the wavefunctions. The orbifold condition projects out the zero mode of the charged Higgs boson and the higher KK mode wavefunctions are purely "trigonometric" of the form in Eq. (13).

4.3 Mass spectrum of the neutral electroweak sector

In the neutral sector, the KK decomposition is complicated by the fact that B_μ and W_μ^3 mix in the bulk as well as on the boundary. In the special case $r_B = r_W$, the bulk and the boundary action can be diagonalized by the same 5 dimensional field redefinition. We present this case first and indicate the generalization to $r_B \neq r_W$ in Section 4.3.2.

4.3.1 The special case $r_B = r_W \equiv r_g$

After electroweak symmetry breaking the 5 dimensional mass matrix in Eq. (1) is diagonalized by the 5 dimensional field redefinition

$$\begin{aligned} Z_M &= \frac{1}{\sqrt{\hat{g}_Y^2 + \hat{g}_2^2}}\left(W_M^3 - B_M\right) \\ A_M &= \frac{1}{\sqrt{\hat{g}_Y^2 + \hat{g}_2^2}}\left(\frac{\hat{g}_Y}{\hat{g}_2}W_M^3 + \frac{\hat{g}_2}{\hat{g}_Y}B_M\right). \end{aligned} \tag{32}$$

If $r_B = r_W \equiv r_g$, this simultaneously diagonalizes the boundary mass terms induced by electroweak symmetry breaking in Eq. (24). The equation of motion and boundary

conditions for the Z_μ gauge field are then

$$\left[\left(\Box - \partial_5^2 + \frac{(\hat{g}_Y^2 + \hat{g}_2^2)\hat{v}^2}{4}\right)\eta^{\mu\nu} - \partial^\mu\partial^\nu\right] Z_\mu = 0 \quad (33)$$

$$\left(\pm\partial_5 + r_g\left[\Box\eta^{\mu\nu} - \partial^\mu\partial^\nu\right] + r_H\frac{(\hat{g}_Y^2 + \hat{g}_2^2)\hat{v}^2}{4}\right) Z_\mu|_{y=\pi R,0} = 0 \quad (34)$$

while those for A_μ are

$$\left[\left(\Box - \partial_5^2\right)\eta^{\mu\nu} - \partial^\mu\partial^\nu\right] A_\mu = 0 \quad (35)$$

$$\left(\pm\partial_5 + r_g\left[\Box\eta^{\mu\nu} - \partial^\mu\partial^\nu\right]\right) A_\mu|_{y=\pi R,0} = 0. \quad (36)$$

Similar to the charged gauge bosons the mass determining relations and wavefunctions are found using the results of Section 3 with the identifications $r_\Phi \to r_g$, $m_\Phi^2 \to (\hat{g}_2^2 + \hat{g}_Y^2)\hat{v}^2/4$, and $m_b^2 \to r_H(\hat{g}_2^2 + \hat{g}_Y^2)\hat{v}^2/4$ for Z_μ and $r_\Phi \to r_g$, $m_\Phi^2 \to 0$, and $m_b^2 \to 0$ for A_μ. Hence the zero mode of the photon is always flat, while the zero mode of the Z will be flat only when $r_H = r_g$. The normalization of the Z and photon is the same as in Eq. (29) with replacement $\hat{g}_2^2 \to 1$ due to the basis chosen in Eq. (32).

Similar to the charged bosons in Section 4.2, the neutral sector contains a physical pseudoscalar degree of freedom. Its equation of motion and boundary conditions are

$$\left(\Box - \partial_5^2 + \frac{(\hat{g}_Y^2 + \hat{g}_2^2)\hat{v}^2}{4}\right) a^0 = 0 \quad (37)$$

$$(a^0 \pm r_H\partial_5 a^0)|_{y=\pi R,0} = 0. \quad (38)$$

The wavefunctions and mass determining equations follow directly from the charged Higgs case discussed in the last section with the replacement $\hat{g}_2^2 \to (\hat{g}_Y^2 + \hat{g}_2^2)$.

4.3.2 The general case: $r_B \neq r_W$

If $r_B \neq r_W$, the field redefinition in Eq. (32) no longer decouples the boundary conditions following from Eq. (24) and, at least for the neutral gauge fields, we have to refine the strategy to find the KK decomposition. Before doing so note that the boundary parameters r_B and r_W in the boundary action Eq. (32) only affect the boundary conditions of the gauge fields. The KK decompositions of the physical Higgs bosons are not affected and therefore remain the same as in the $r_B = r_W$ case discussed in the last section.

Aside from the mixing of $B_\mu - W_\mu^3$, the KK decomposition for W_μ^3 is identical to those of $W^\pm$ discussed in Section 4.3.1. The analogous solutions for the B_μ are also given by the substitutions $r_W \to r_B$ and $\hat{g}_2 \to \hat{g}_Y$ for the relations in Section 4.3.1. The mixing term in the bulk $\propto \hat{v}^2 B_\mu W^\mu$ and on the brane $\propto r_H\hat{v}^2 B_\mu W^\mu$ induce off-diagonal terms in the neutral gauge boson mass matrix of the form

$$\mathcal{M}_{m,n}^2 = \frac{\hat{v}^2}{4}\int_0^{\pi R} dy f_n^W(y) f_m^B(y)[1 + r_H(\delta(y) + \delta(y - \pi R))] \quad (39)$$

where $f_n^W(y)$ and $f_m^B(y)$ are the W_μ^3 and B_μ wavefunctions respectively. The even (odd) modes of B_μ only have a non-zero overlap with the even (odd) modes of W_μ^3, thereby

still preserving KK parity. In particular there is a non-trivial overlap between the zero mode of the B_μ gauge boson and all even modes of the W^3_μ gauge boson. In order to find the exact mass spectrum and wavefunctions of the neutral sector, the full KK mass matrix in the neutral sector has to be diagonalized.

4.4 Modifications of zero mode and KK mode couplings

Using the wavefunctions and mass spectra for all electroweak fields derived in the last section, we can calculate the couplings of all KK particles by integrating out the extra dimension.

The coupling of fermions to the W or B bosons arise from the 5 dimensional action

$$S = \int d^5x \overline{f} \gamma^M D_M f \tag{40}$$

where D_M is appropriate covariant derivative. Assuming that fermions have no BLTs, the couplings are

$$g^f_{i,lmn} = \int dy f^{W,B}_l f^f_m f^f_n \tag{41}$$

where $i = B, W$ and $\{f^f_m\}$ is the wavefunction of the m^{th} KK mode. In particular, the couplings of the zero modes are given by

$$g^f_{i,000} = \frac{1}{\pi R} \int dy f^{W,B}_0, \tag{42}$$

where we used that the fermion zero modes are constant in the absence of fermion BLTs.

Now, let us consider the triple and quartic gauge boson vertices of the $SU(2)$. They follow from the overlap integrals

$$g^t_{2,lmn} = \int dy f^W_l f^W_m f^W_n \left(1 + r_W \left[\delta(y) + \delta(y - \pi R)\right]\right]) \tag{43}$$

$$\left(g^q_{2,klmn}\right)^2 = \int dy f^W_k f^W_l f^W_m f^W_n \left(1 + r_W \left[\delta(y) + \delta(y - \pi R)\right]\right]). \tag{44}$$

For generic values of r_W it is obvious that $g^f_{i,000} \neq g^t_{2,000} \neq g^q_{2,0000}$. As the zero mode level is identified with the Standard Model, the BLKTs induce a modification to the WWZ vertex.

The vertices of the Higgs KK modes with gauge bosons and fermions are calculated analogously from overlap integrals, taking the BLTs into account as in Eq. (43) and Eq.(44). Using the mass determining equations and wavefunctions of the previous subsections, for fixed (R, r_B, r_W, r_H) we can match the zero mode spectrum and couplings to those of the Standard Model and hence determine the spectrum and coupling of the higher KK modes.

5 Phenomenology of Electroweak BLTs in UED

As shown in the last section, BLTs can significantly modify the KK spectrum and gauge couplings in UED. The modification of the spectrum can alter the nature of the lightest KK particle so that $B^{(1)}$ is no longer the LKP. However these BLTs can also affect the zero mode couplings and masses and therefore are constrained by experiment.

In this section we study the constraints on r_B, r_W, and r_H arising from matching the zero mode spectrum of non-minimal UED to that of the Standard Model. We adopt the strategy of fixing the parameters (r_B, r_W, r_H, R) and solving for the 5 dimensional quantities $(\hat{g}_Y, \hat{g}_2, \hat{v})$ in terms of the Standard Model observables $\alpha_{em}, G_F, m_Z, m_W$. Therefore the 5 dimensional quantities $(\hat{g}_Y, \hat{g}_2, \hat{v})$ are over constrained and provide a bound on the parameters (r_B, r_W, r_H, R). A further potential bound arises from the LEP measurement of the WWZ vertex.

In this article we discuss three qualitatively differing regions of the non-minimal UED parameter space. The first parametric scenario is one in which all the electroweak boundary localized kinetic terms are uniform and all other Higgs boundary terms are zero. In this scenario the LKP is the KK photon where the Weinberg angle is the same at every KK level. However as KK number is explicitly broken by the BLKTs, the even KK modes of $W^{\pm}$ and Z have non-zero couplings to the zero mode fermions which leads to non-trivial contributions to the Fermi constant G_f.

The second parametric scenario we consider in Section 5.2 is the case $r_g \equiv r_W = r_B \neq r_H$, with all other Higgs BLTs zero. As r_H is split from r_g, the zero mode wavefunctions of the gauge bosons are not flat which leads to modified gauge couplings. We calculate the bounds on $r_H - r_g$ arising from modifications of the zero mode mass spectrum. In this scenario we find regions of parameter space in which $h^{(1)}$ is the LKP.

The third scenario we consider in Section 5.3, is the case in which $r_W \neq r_B = 0 = r_H$ and all the other Higgs brane terms are zero. As $r_W \neq r_B$, the bulk and brane mass terms of the neutral gauge boson sector induce mixing between different KK levels of the B gauge boson and the the W^3 gauge boson. For large enough r_W the $W^{3(1)}$ becomes lighter than the $B^{(1)}$, in which case the LKP becomes mainly $W^{3(1)}$. As for the previous scenarios, we determine bounds on r_W which arise due to the modified zero mode couplings. We show that within these bounds, a $W^{3(1)}$ LKP can easily be realized.

5.1 Scenario I: $r_W = r_B = r_H$

For a start, let us consider the special case of uniform gauge BLKTs $r_{EW} \equiv r_W = r_B = r_H$. Assuming the absence of boundary terms for the fermions and for the gluon, this model presents a simple extension of UED with only four free parameters R, r_{EW}, μ_b, m_h. For simplicity, we assume $\mu_b = 0$ and $m_h = 115$ GeV.[10] For uniform r_{EW}, the boundary conditions on the gauge fields imply that all gauge field zero modes are flat. Therefore the matching of the underlying 5 dimensional parameters $\hat{g}_Y, \hat{g}_2, \hat{v}$ to the Standard Model

[10] Relaxing these assumption results in heavier Higgs KK masses, but otherwise does not affect the mass spectrum.

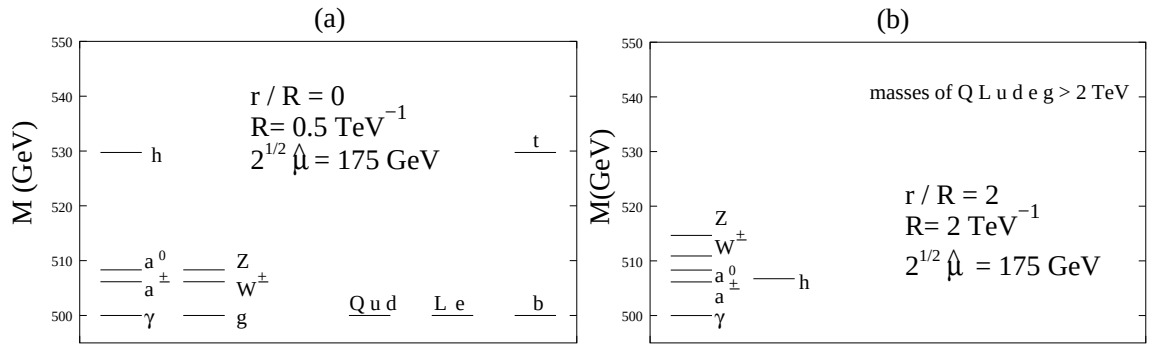

Figure 2: Sample spectra for UED. (a) The tree level UED spectrum without BLTs (first KK level) for $R^{-1} = 500$ GeV. (b) The tree level UED spectrum with $r_B = r_W = r_H = 2R$, $\mu_b = 0$, $R^{-1} = 1$ TeV and $m_h = 115$ GeV. Parameters are chosen such that the LKP masses of both model coincide.

values g_Y, g_2, v is similar to "standard" UED, with $\pi R \to \pi R + 2r_{EW}$ in the rescaling of the couplings, but the identification of $\hat{\mu}$ with m_h is altered. At the first KK level, the fermions and gluon have a mass $\sim n/R$ but the gauge bosons and Higgs masses are reduced to lower values. Thus R^{-1} determines the fermion and gluon mass scale, while r_{EW} can be thought of as parameterizing the mass splitting between the electroweak KK modes and the fermion and gluon KK modes. In Fig. 2 we show the effect of r_{EW} on the particle spectrum of UED. Fig. 2(a) corresponds to "standard" UED with $R^{-1} = 0.5$ TeV while Fig. 2(b) corresponds to the uniform r_{EW} scenario with $\mu_b = 0, r_{EW}/R = 2$ and $R^{-1} = 1$ TeV. In spite of different values of R it is possible to choose r_{EW}/R, such that the LKP mass is the same in both scenarios.

From the equations of motion and boundary conditions in Sections 4.1, 4.2 and 4.3.1 we can see that for uniform BLKTs the spectrum has the following structure

$$m_{Z^{(1)}} \geq m_{a^{0(1)}} > m_{a^{\pm(1)}} > m_{\gamma^{(1)}} \tag{45}$$

$$m_{Z^{(1)}} > m_{W^{\pm(1)}} \geq m_{a^{\pm(1)}} \tag{46}$$

$$m_h^{(1)} > m_{\gamma^{(1)}}. \tag{47}$$

Hence, the LKP is always the KK photon or, more precisely, the linear combination $\gamma^{(1)} = \sin(\theta_W^{(1)})B^{(1)} + \cos(\theta_W^{(1)})W^{3(1)}$, where for uniform r_{EW} the Weinberg angle $\theta_W^{(n)}$ at all KK levels is identical to that of the Standard Model.

As the BLTs do not introduce any extra sources flavor violation and the fermion KK modes are heavier than in "standard" UED, the UED GIM mechanism [7] implies weaker flavor constraints. As the Weinberg angle is the same at every KK level, the LKP can annihilate efficiently through a t-channel $W^{(1)}$ into W^+W^- even if the KK fermions are quite heavy. In the limit of very heavy KK fermions, the requirement that the KK photon does not overclose the universe implies an upper bound on LKP mass of about 1.6 TeV. This bound is a constraint on the LKP mass which can be substantially smaller than the compactification scale R^{-1}.

The collider constraints and electroweak constraints can be strong in this scenario.

As KK number is explicitly broken by the BLTs, higher KK level gauge bosons have non-zero couplings to the zero mode fermions. Hence there are electroweak corrections even at tree level. For example, the Fermi constant G_f obtains contributions from the exchange of all even $W^{\pm(n)}$ KK modes. In the next section, we study constraints arising from the tree level modifications of the zero mode and KK mode couplings in detail.

5.1.1 Electroweak constraints

In order to determine constraints from the electroweak sector we first match the zero mode spectrum on to the Standard Model, using the results of Sections 4.1, 4.2 and 4.3.1. We perform the matching by demanding that $\hat{g}_2, \hat{g}_Y$ and $\hat{v}$ are chosen so that α, G_f, m_W and m_Z have their correct values within experimental errors, for fixed r_{EW} and R. As there are three underlying parameters and four Standard Model quantities, the system is over constrained. Hence we can predict one of the Standard Model parameters which we use to constrain the input parameters r_{EW} and R.

For uniform r_{EW} the gauge boson zero modes are flat and their masses are directly related to the 5 dimensional parameters by

$$m_W^2 = \hat{m}_W^2 \equiv \frac{\hat{g}_2^2 \hat{v}^2}{4} \tag{48}$$

$$m_Z^2 = \hat{m}_Z^2 \equiv \frac{(\hat{g}_2^2 + \hat{g}_Y^2)\hat{v}^2}{4}, \tag{49}$$

giving us two relations between the 4 dimensional and 5 dimensional parameters. With $\hat{m}_W$ and $\hat{m}_Z$ determined, all $W^\pm$ and Z KK mode wavefunctions and masses are can be found by numerically solving the mass determining equations given in Sections 4.1, 4.2 and 4.3.1 which are summarized in Eq. (126) in Appendix C.

The Fermi constant G_f gets contributions from the exchange of the $W^{\pm(0)}$ mode as well as higher even KK modes. Summing over all W KK modes that have non-zero couplings to the zero mode fermions we find the effective Fermi constant

$$G_f = \frac{\hat{g}_2^2}{4\sqrt{2}\pi R} \sum_{n=0}^{\infty} \frac{b_{2n}}{m_{W^{(2n)}}^2} \tag{50}$$

where

$$b_0 = \frac{1}{1 + \frac{2r_{EW}}{\pi R}}, \tag{51}$$

$$b_{2n} = \left(\frac{8 \sin^2 \frac{M_{2n}^W \pi R}{2}}{\left(1 + \frac{\sin M_{2n}^W \pi R}{M_{2n}^W \pi R} + \frac{4r_{EW}}{\pi R} \cos^2 \frac{M_{2n}^W \pi R}{2}\right) (M_{2n}^W \pi R)^2} \right), \tag{52}$$

$M_{2n}^W = m_{W^{\pm(2n)}}^2 - \hat{m}_W^2$, and $m_{W^{\pm(2n)}}$ are the physical masses of the $W^\pm$ KK modes.

The $U(1)_{em}$ coupling in terms of the the 5 dimensional couplings is

$$\alpha_{em} = \frac{1}{4\pi(\pi R + 2r_{EW})} \frac{\hat{g}_Y^2 \hat{g}_2^2}{\hat{g}_Y^2 + \hat{g}_2^2}. \tag{53}$$

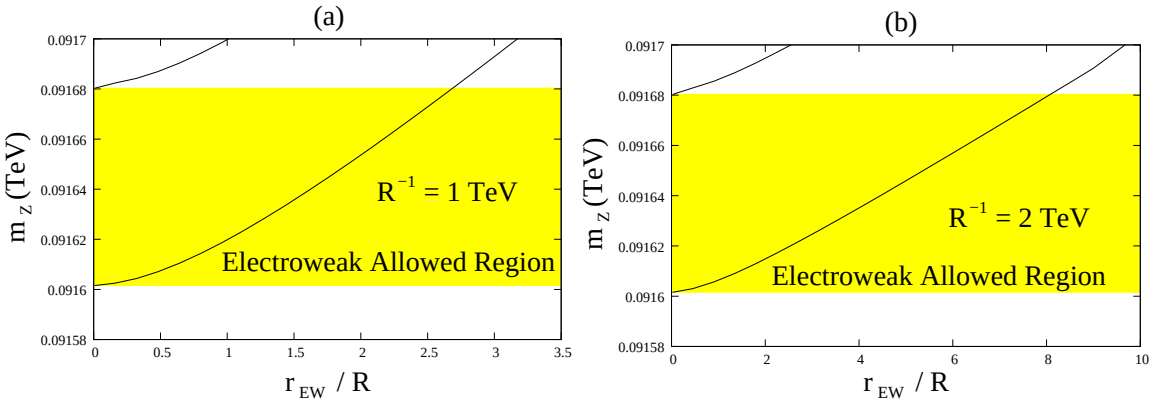

Figure 3: Variation of m_Z^{nUED} for different values of r_{EW} with $R^{-1} = 1$ TeV and $R^{-1} = 2$ TeV. The yellow (gray) band corresponds to the 2σ allowed tree-level value of m_Z^{tree}. The region within the black lines is the 2σ predicted tree-level value of m_Z^{nUED}.

where the factor $\pi R + 2r_{EW}$ comes from the normalization of the gauge boson zero modes with BLKTs r_{EW}.

As we are studying the tree level corrections to the Standard Model relations, we fix the values of $\alpha = 1/(127.925 \pm 0.016)$, $m_W = (80.398 \pm 0.025)$ GeV and $G_f = (11.66367 \pm 0.00005)$ TeV^{-2} [24] and use Eq. (48), Eq. (50), and Eq. (53) to predict the value of $m_Z^{nUED}(R, r_{EW}, m_W, G_f, \alpha)$ and compare it to

$$\begin{aligned} \lim_{R, r_{EW} \to 0} m_Z^{nUED}(R, r_{EW}, m_W, G_f, \alpha) &\equiv m_Z^{tree}(m_W, G_f, \alpha) \\ &= m_Z^{exp} - m_Z^{SM}|_{loop}(m_W, G_f, \alpha), \end{aligned} \tag{54}$$

where m_Z^{exp} is the experimentally measured Z mass while $m_Z^{SM}|_{loop}(m_W, G_f, \alpha)$ is the Standard Model loop contribution to the Z mass. Therefore we can translate all experimental uncertainties into a band of allowed values of $m_Z^{tree}(m_W, G_f, \alpha)$ and compare it to the predicted band of values for the tree level nUED Z mass $m_Z^{nUED}(R, r_{EW}, m_W, G_f, \alpha)$.

Fig. 3 presents the effect of varying r_{EW} on the predicted value of m_Z^{nUED} for $R^{-1} = 1$ TeV and $R^{-1} = 2$ TeV, assuming a 2σ error in the input values of α, m_W and G_f. From Fig. 3 we see that the constraints on r_{EW} are weaker for increasing R^{-1}. For $R^{-1} = 1$ TeV the electroweak constraints force $r_{EW}/R < 2.7$ while for $R^{-1} = 2$ TeV the bound only lies at $r_{EW}/R < 8.0$. Thus for large compactification scales we can split the fermion KK modes (with $m_f^{(1)} \sim 1/R$) from the gauge and Higgs KK modes. Also note, that a higher compactification scale does *not* necessarily imply a heavier $\gamma^{(1)}$ LKP as can be seen from the sample spectrum in Fig. 2.

5.2 Scenario II: $r_W = r_B \equiv r_g < r_H$

For uniform r_{EW}, the KK photon always remains the LKP, so to change the nature of the LKP we need to split the BLKTs. As a next step let us consider a scenario in which

we vary the Higgs BLKT while keeping the gauge BLKTs equal at $r_B = r_W \equiv r_g$. For $r_g > r_H$, it is obvious that the LKP remains the KK photon as the gauge boson KK mode masses are reduced relative to the Higgs. We therefore focus on the choice $r_g < r_H$ for which it is conceivable that the $h^{(1)}$ becomes lighter than the KK photon.

For $r_H \neq r_g$, the gauge boson zero modes are not flat. We thus need to find the correct values of $\hat{g}_Y, \hat{g}_2$ and $\hat{v}$ so as to match the zero mode spectrum to that of the Standard Model. As in Section 5.1.1, we perform the matching by demanding the correct values for α, G_f, m_W and determine the tree-level value for m_Z^{nUED}, which leads to a bound on r_g and r_H. In Sec. 5.2.1 we derive the relations between the Standard Model parameters α, G_f, m_W, m_Z and the underlying parameters $(\hat{g}_Y, \hat{g}_2, \hat{v})$ to study the constraints on (r_g, r_H, R). In Sec 5.2.2, we use this information in order to determine the LKP in this scenario and show that there exist regions of parameter space where $h^{(1)}$ is the LKP.

5.2.1 Electroweak constraints

We work in the $A - Z$ basis defined in Eq. (32). From the appropriate substitutions in Eq. (126) for $W^\pm$ and Z, the physical masses $m_{I^{(n)}}$ satisfy the condition[11]

$$\frac{r_g (M_n^I)^2 - (r_H - r_g)\hat{m}_I^2}{M_n^I} = -\tan\frac{M_n^I \pi R}{2} \tag{55}$$

where $I = (W, Z)$, $\hat{m}_Z^2 = (\hat{g}_2^2 + \hat{g}_Y^2)\hat{v}^2/4$, $\hat{m}_W^2 = \hat{g}_2^2\hat{v}^2/4$ and $M_n^I = \sqrt{\hat{m}_I^2 - m_{I^{(n)}}^2}$.

As in the uniform r_{EW} scenario, the effective Fermi constant obtains contributions from the exchange of all even $W^\pm$ KK modes as given earlier in Eq. (50) with the non-zero KK coefficients b_{2n} as given in Eq. (52) with $r_{EW} \to r_g$. Due to the non-flat zero mode profile, Eq. (52) also holds for the zero mode contribution b_0 in this scenario. Furthermore, working in the basis of Eq. (32), it is obvious that the boundary mass term of the photon vanishes. Hence the relation between the $U(1)_{em}$ coupling and the 5 dimensional couplings is again given by Eq. (53) with $r_{EW} \to r_g$.

To determine the allowed parameter space in (r_H, r_g, R) we calculate $\hat{m}_W$ by fixing the zero mode W mass and using Eq. (55). Once we have found $\hat{m}_W$ we are able to determine all W KK masses and use Eq. (50) to determine $\hat{g}_2$. $\hat{v}$ is determined via the definition of $\hat{m}_W \equiv \hat{g}_2\hat{v}/2$. Finally, using Eq. (53) we can determine $\hat{g}_Y$ in terms of $\hat{g}_2$. m_Z is fixed by the parameter set $(r_g, r_H, R, \hat{g}_Y, \hat{g}_2, \hat{v})$ and a comparison with the experimental values yields a constraint on (r_g, r_H, R). Again using the electroweak values of $\alpha = 1/(127.925 \pm 0.016)$, $m_W = (80.398 \pm 0.025)$ GeV and $G_f = (11.66367 \pm 0.00005)$ TeV^{-2} we can predict the tree-level m_Z^{nUED} value.

Fig. 4 shows the resulting predictions of the lower edge of the $m_Z^{nUED}(R, r_g, r_H)$ band for compactification scales of $R^{-1} = 1$ and 2 TeV. The different contours correspond to fixed values of r_g/R and varying values of $\Delta r/R \equiv (r_H - r_g)/R$. The yellow (gray) band corresponds to the 2σ allowed values of m_Z^{tree}. For a given value of r_g/R the bound on Δr

[11] For our parameter choice of $r_H > r_g$ the hyperbolic mass conditions in Eq. (126) do not have a solution, such that the zero mode in this case is given by a cosine solution as well.

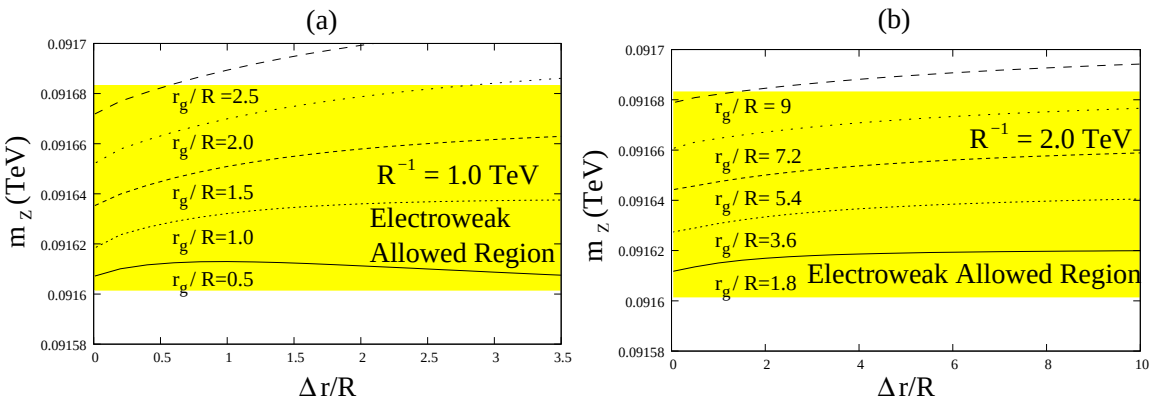

Figure 4: Constraints on r_g/R and $\Delta r/R \equiv (r_H - r_g)/R$ from tree level corrections to the Z mass for (a) $R^{-1} = 1$ TeV and (b) $R^{-1} = 2$ TeV. We plot the lower edge of the $m_Z^{nUED}(R, r_g, r_H)$ band for different values of r_g/R. The yellow (gray) band corresponds to the 2σ allowed values of m_Z^{tree} as defined in Eq. (54). For a given value of r_g/R the bound on Δr can be inferred from the intersection of the corresponding contour line with the upper bound of the yellow (gray) band.

can be inferred from the intersection of the corresponding contour line with the upper bound of the yellow (gray) band. As can be seen, for moderate values of r_g substantial splittings between r_g and r_H are allowed.

The analysis presented here can be extended to other Standard Model observables which get modified at tree level. For example from Eqs. (43) and Eq. (44) it can be seen that the WWZ vertex and the $WWWW$ vertex are modified. We performed the full analysis for the WWZ vertex and found that it leads to constraints which are substantially weaker than the constraints from m_Z presented above. This is to be expected as the experimental precision on α, G_f, m_W, m_Z is much higher than the precision on the WWZ vertex [24]. Similarly, we expect the bounds from the $WWWW$ vertex to be sub-dominant.

5.2.2 Determining the LKP

With $(\hat{g}_Y, \hat{g}_2, \hat{v})$ fixed by matching to the Standard Model parameters for a given set of (r_g, r_H, R), the mass determining equations in Eq. (126) fix the KK spectrum of all particles in the electroweak sector. From Eq. (126) it follows that

$$\begin{aligned} m_{Z^{(1)}} &\geq m_{a^{0(1)}} > m_{a^{\pm(1)}} \\ m_{Z^{(1)}} &> m_{W^{\pm(1)}} \geq m_{a^{\pm(1)}} \\ m_{W^{\pm(1)}} &> m_{\gamma^{(1)}} \end{aligned} \tag{56}$$

leaving $\gamma^{(1)}, a^{\pm(1)}$ and $h^{(1)}$ as possible LKPs. From Section 4.3.1, the mass of the KK photon is determined by

$$r_g m_{\gamma^{(1)}} = \cot \frac{m_{\gamma^{(1)}} \pi R}{2}. \tag{57}$$

From Section 4.2, the mass of the $a^{\pm(1)}$ is

$$m^2_{a^{\pm(1)}} = \frac{\hat{g}_2^2 \hat{v}^2}{4} + (M_{a^{\pm(1)}})^2, \tag{58}$$

where $M_{a^{\pm(1)}}$ satisfies the equation

$$r_H M_{a^{\pm(1)}} = \cot \frac{M_{a^{\pm(1)}} \pi R}{2}. \tag{59}$$

While all other KK spectra in the electroweak sector are fixed, the KK spectrum of the Higgs depends on $\hat{\mu}$ and μ_b. In order to be able to compare the masses of the $a^{\pm(1)}$ and the $h^{(1)}$, we assume $\mu_b = 0$ and fix $\hat{\mu}$ by demanding that the zero mode Higgs mass is fixed at $m_h = 115$ GeV. With these choices, the mass of the KK Higgs $m_{h^{(1)}}$ satisfies the constraint

$$\frac{r_H m^2_{h^{(1)}}}{\sqrt{m^2_{h^{(1)}} - 2\hat{\mu}^2}} = \cot \left(\frac{\sqrt{m^2_{h^{(1)}} - 2\mu^2} \pi R}{2} \right), \tag{60}$$

where $\hat{\mu}$ is determined from

$$\frac{r_H m_h^2}{\sqrt{2\hat{\mu}^2 - m_h^2}} = \tanh \left(\frac{\sqrt{2\hat{\mu}^2 - m_h^2} \pi R}{2} \right). \tag{61}$$

Using these equations, we calculate the KK masses for the $h^{(1)}$, $a^{\pm(1)}$ and $\gamma^{(1)}$ to find the LKP in the parameter space $(r_g, \Delta r)$. Fig. 5 shows the resulting LKP phase diagrams for $R^{-1} = 1$ and 2 TeV. The red (dark gray) areas are excluded by the electroweak fit derived in the last section. For negative Δr (not displayed) and in the green (shaded) region at low Δr the LKP is the KK photon. In the yellow (gray) area either the LKP is the $a^{\pm(1)}$ or the zero mode Higgs mass is less than 115 GeV. Therefore the yellow (gray) region is experimentally disfavored. The white triangular area signifies the maximally allowed parameter space with a Higgs LKP. Assuming that $\mu_b \neq 0$ or $m_h > 115$ GeV makes the first KK Higgs heavier and thus reduces the Higgs LKP parameter space further.

While for $R^{-1} = 1$ TeV the Higgs LKP parameter space is strongly constrained, it opens up for a larger compactification scales as can be seen in Fig. 5(b). We emphasize again that a higher compactification scale does not imply a substantially heavier LKP. In Fig. 5(a) and (b), we give three sample points at the corners of the Higgs LKP parameter space with their respective $h^{(1)}$ masses. The Higgs LKP mass for $R^{-1} = 1$ TeV lies in a range of 440 GeV $\lesssim m_{h^{(1)}} \lesssim$ 460 GeV, while for $R^{-1} = 2$ TeV the allowed Higgs LKP mass lies in the range of 490 GeV $\lesssim m_{h^{(1)}} \lesssim$ 830 GeV.

In Fig.6 (a) and (b), we show the first KK level masses of the sample points A and C for $R^{-1} = 2$ TeV as defined in Fig.5 (b). As is expected, the masses of $a^{\pm(1)}$ and $h^{(1)}$ at these points are almost degenerate. The masses of the KK gauge bosons lie higher because $r_H > r_g$. Comparing sample points A and C, point A lies at larger r_H and r_g. Therefore the mass scale for all electroweak particles is lower than at point C. As $r_H - r_g$ is larger at point A, the relative splitting between the Higgs KK masses and the gauge boson KK masses is larger than at point C. The fermion and gluon KK mode masses remain at the compactification scale.

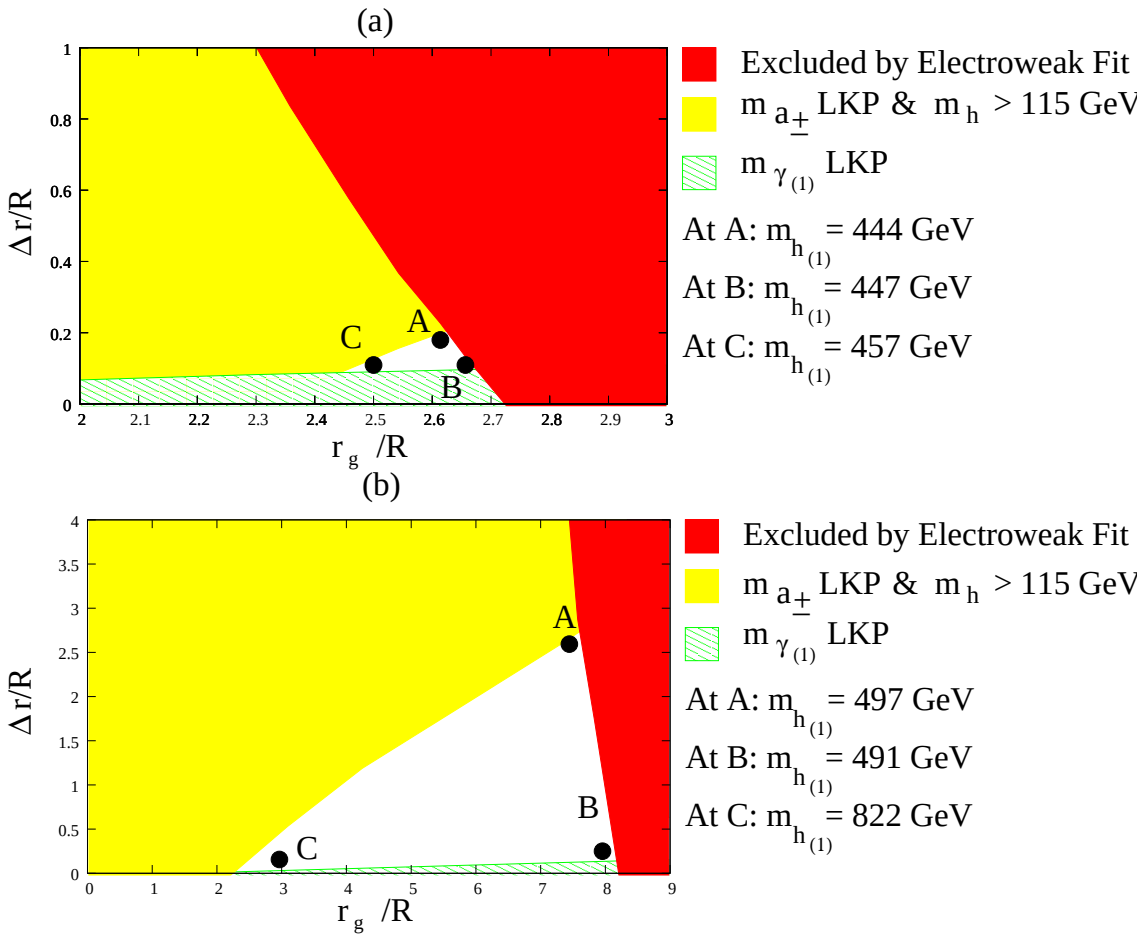

Figure 5: LKP phase space in the $r_g \equiv r_B = r_W \neq r_H$ scenario. For (a) $R^{-1} = 1$ TeV and (b) $R^{-1} = 2$ TeV, we plot the regions of different types of LKP in the $\Delta r/R \equiv (r_H - r_g)/R$ versus r_g/R plane. The Higgs brane mass parameter has been set to $\mu_b = 0$ and the zero mode Higgs mass has been set to 115 GeV. The red (dark gray) region is excluded by the electroweak constraints in Section 5.2.1. In the yellow(gray) region the LKP is the $a_{\pm(1)}$ while in the green (shaded) region the KK photon is the LKP. In the white region the LKP is the KK Higgs. The points A, B and C in each plot represent sample points with a Higgs LKP whose mass is given on the right of the plots.

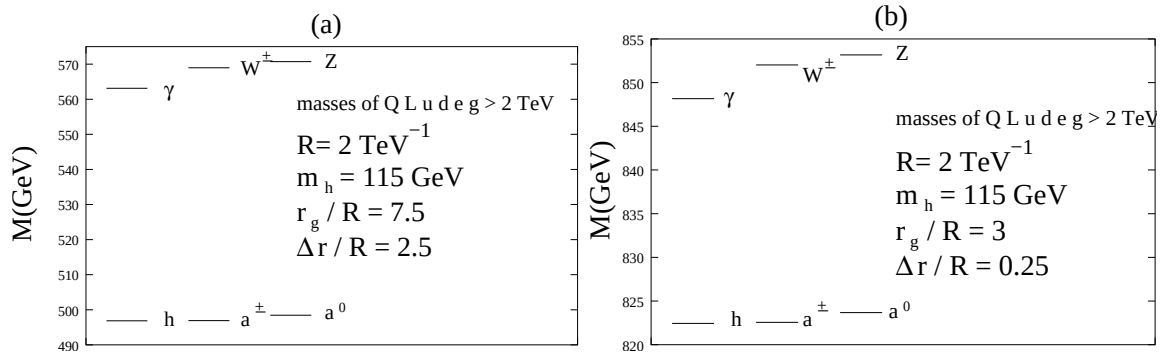

Figure 6: Sample spectra for UED with $r_g \neq r_H$. (a) The tree level UED spectrum with $R^{-1} = 2$ TeV, $r_g \equiv r_B = r_W = 7.5R$ and $\Delta r \equiv r_H - r_g = 2.5R$ which corresponds to sample point A of Fig. 5(b). (b) The tree level UED spectrum with $R^{-1} = 2$ TeV, $r_g = 3R$ and $\Delta r = 0.25R$ which corresponds to sample point C of Fig. 5(b).

5.3 Scenario III: $r_w \neq r_B$

As a third example we investigate a scenario with $r_B \neq r_W$. As we showed, boundary kinetic terms reduce the KK masses. Therefore setting $r_W > r_B$ is an easy way to obtain a $W^{3(1)}$-like LKP. To see qualitatively how the LKP is changed in this scenario, consider the mass matrix at the first KK level

$$M^2_{B^{(1)},W^{3(1)}} = \begin{pmatrix} m^2_{B^{(1)}} & \mathcal{M}^2_{1,1} \\ \mathcal{M}^2_{1,1} & m^2_{W^{(1)}} \end{pmatrix}, \tag{62}$$

where the mixing elements $M^2_{m,n}$ have been defined in Eq. (39). To a good approximation, the LKP is the lighter eigenstate of this $B^{(1)} - W^{3(1)}$ system. If we choose a sufficiently large r_W then we can make $m^2_{W^{(1)}} < m^2_{B^{(1)}}$, in which case $W^{3(1)}_\mu$ becomes the main component of lighter eigenstate of the $B^{(1)}_\mu - W^{3(1)}_\mu$ system.

However this is not the full story. As indicated in Sec. 4.3.2 for $r_W \neq r_B$, the KK basis $\{f^B_n\}$ and $\{f^W_n\}$ differ and electroweak symmetry breaking induces $B - W^3$ mixing between different KK levels as given in Eq. (39).

To address the KK mode mixing qualitatively, consider the only non-vanishing mass matrix elements which mix B and W^3,[12]

$$M^2_{B^{(2m)},W^{3(2n)}} = \begin{pmatrix} m^2_{B^{(2m)}} & \mathcal{M}^2_{2m,2n} \\ \mathcal{M}^2_{2m,2n} & m^2_{W^{3(2n)}} \end{pmatrix}. \tag{63}$$

In the presence of BLTs, the mass difference is of the order

$$m^2_{B^{(2m)}} - m^2_{W^{3(2n)}} \sim \left(\frac{2n}{R}\right)^2 - \left(\frac{2m}{R}\right)^2 = \frac{4(m^2 - n^2)}{R^2} \tag{64}$$

[12]We give the argument for even KK modes, here. The same holds true for odd KK mode mixing. Mixing between even and odd modes is forbidden by KK parity.

if $m \neq n$, but the normalization of the wavefunctions in the extra dimension puts a bound on these mixing terms

$$\mathcal{M}^2_{2m,2n} < \frac{\hat{g}_Y \hat{g}_2 \hat{v}^2}{4}. \tag{65}$$

Hence the KK mode mixing between the $B^{(n)}$ and $W^{(m)}$ modes satisfies

$$\sin^2 \theta_{mn} \lesssim \frac{\left(\frac{\hat{g}_Y \hat{g}_2 \hat{v}^2}{4}\right)^2}{\frac{4(m^2-n^2)m^2}{R^4}}, \tag{66}$$

which is small whenever $R^{-1} >> \frac{\hat{g}_Y \hat{g}_2 \hat{v}^2}{4}$ and $m \neq n$. The largest mixing of modes between the B and W KK towers occurs when $m = n$, and to good approximation, the mass matrix can be diagonalized KK level by KK level, underlining the validity of the qualitative argument on a $W^{3(1)}$ LKP given above. We perform a quantitative study of obtaining a $W^{3(1)}$ LKP via BLTs in Section 5.3.2 in which we take the KK mode mixing into account numerically.

From the above discussion it is clear that the zero modes mix with higher KK modes as well. Matching the zero mode sector on to the Standard Model is therefore non-trivial. In the next section, we numerically diagonalize the neutral gauge sector mass matrix and follow the same procedure as in Sections 5.1.1 and 5.2.1 in order to determine electroweak constraints on r_W.

5.3.1 Electroweak constraints

To perform a quantitative study of the LKP we choose the special case $r_W \neq 0 = r_B = r_H$. As outlined in Section 4.3.2 the equations of motion and boundary conditions for W are

$$\left[\left(\Box - \partial_5^2 + \frac{\hat{g}_2^2 \hat{v}^2}{4}\right)\eta^{\mu\nu} - \partial^\mu \partial^\nu\right] W^3_\nu = 0 \tag{67}$$

$$\left(\pm\partial_5 + r_W\left[\Box\eta^{\mu\nu} - \partial^\mu\partial^\nu\right]\right) W^3_\nu|_{y=\pi R,0} = 0 \tag{68}$$

and for B are

$$\left[\left(\Box - \partial_5^2 + \frac{\hat{g}_Y^2 \hat{v}^2}{4}\right)\eta^{\mu\nu} - \partial^\mu \partial^\nu\right] B_\nu = 0 \tag{69}$$

$$\pm\partial_5 B_\nu|_{y=\pi R,0} = 0. \tag{70}$$

Hence we expand $W^{(3)}_\mu$ in the basis for a gauge field with BLKTs and (as we chose $r_B = 0$) we expand B_μ in the "standard" UED basis. However, as $W^{(3)}_\mu$ and B_μ are not the mass eigenstates of the bulk Lagrangian with electroweak symmetry breaking, the term $\hat{v}^2 W^\mu B_\mu$ induces the mass mixings given in Eq.(39).

For the charged gauge field sector, from Eq. (126) the zero mode mass is $m^{(0)}_W$ is determined by

$$\frac{r_W m^2_{W^{(0)}}}{\sqrt{m^2_{W^{(0)}} + \hat{m}^2_W}} = \tanh \frac{\sqrt{m^2_{W^{(0)}}) + \hat{m}^2_W}\pi R}{2}. \tag{71}$$

Turning this relation around we can determine $\hat{m}_W$ by setting $m_W^{(0)} \equiv m_W$. With $\hat{m}_W$ determined, the mass spectrum of $W^{\pm(n)}$ is fixed. As in Sections 5.1.1 and 5.2.1, $\hat{g}_2$ can be determined by calculating the effective Fermi constant from Eq. (50), where the non-zero $W^\pm$ KK mode contributions b_{2n} are given by Eq. (52) with $r_{EW} \to r_W$ while the hyperbolic zero mode implies

$$b_0 = \frac{8 \sinh^2 \frac{M_{2n}^W \pi R}{2}}{\left(1 + \frac{\sinh M_{2n}^W \pi R}{M_{2n}^W \pi R} + \frac{4 r_W}{\pi R} \cosh^2 \frac{M_{2n}^W \pi R}{2}\right) \left(M_{2n}^W \pi R\right)^2}. \tag{72}$$

The above results enable us to determine $\hat{g}_2$ and $\hat{v}$ from the charged sector for a given set of parameters R, r_W. The next goal is to calculate α and use it as a matching condition for $\hat{g}_Y$. In Sections 5.1.1 and 5.2.1, we were able to give an explicit and easily invertible relation for $\alpha(R, r_g, r_H, \hat{g}_Y, \hat{g}_2)$. For $r_W \neq r_B$, this task is complicated by the fact that the photon is only determined implicitly as the lightest eigenstate of the neutral gauge boson mass matrix.

The relationship between the 4 dimensional mass eigenstates and the original $B-W$ basis is

$$\begin{aligned}
A^{(0)} &= U_{1j}^T \mathcal{B}^j && (73)\\
Z^{(0)} &= U_{2j}^T \mathcal{B}^j && (74)\\
A^{(1)} &= U_{3j}^T \mathcal{B}^j, && (75)\\
Z^{(1)} &= U_{4j}^T \mathcal{B}^j, && (76)\\
&\vdots
\end{aligned}$$

where $\mathcal{B}^j$ denotes $(B^{(0)}, W^{3(0)}, B^{(1)}, W^{3(1)}, ...)^T$.

In order to determine the basis transformation U_{ij}. We start from a trial value of $\hat{g}_Y$. Together with the already determined values of $\hat{g}_2$ and $\hat{v}$, we calculate the neutral gauge boson mass mixing matrix. As we work in the $B-W$ basis, the $W^{3(m)} - W^{3(n)}$ and $B^{(m)} - B^{(n)}$ mixing terms are zero for $m \neq n$. The diagonal elements are given by $m^2_{W^{(n)}}$ and $m^2_{B^{(n)}}$, while the $B^{(n)} - W^{(m)}$ mixing is described in Eq. (39). We numerically diagonalize the trial mass matrix to obtain U_{ij}. Eq. (73) then determines the photon in the $B-W$ basis. The couplings of the zero mode photon to zero mode fermions can be derived from the 5 dimensional action

$$\begin{aligned}
S &\supset \int d^4x dy\, i\, \overline{e}_R \gamma^M B_M e_R \supset \int d^4x\, i\, Q_{e_R} \overline{e}_R^{(0)} \gamma^\mu A_\mu e_R^{(0)}\\
S &\supset \int d^4x dy\, \frac{i}{2} \overline{e}_L \gamma^M B_M e_L + \frac{i}{2} \overline{e}_L \gamma^M W_M^3 e_L\\
&\supset \int d^4x\, i\, Q_{e_L} \overline{e}_L^{(0)} \gamma^\mu A_\mu^{(0)} e_L^{(0)},
\end{aligned} \tag{77}$$

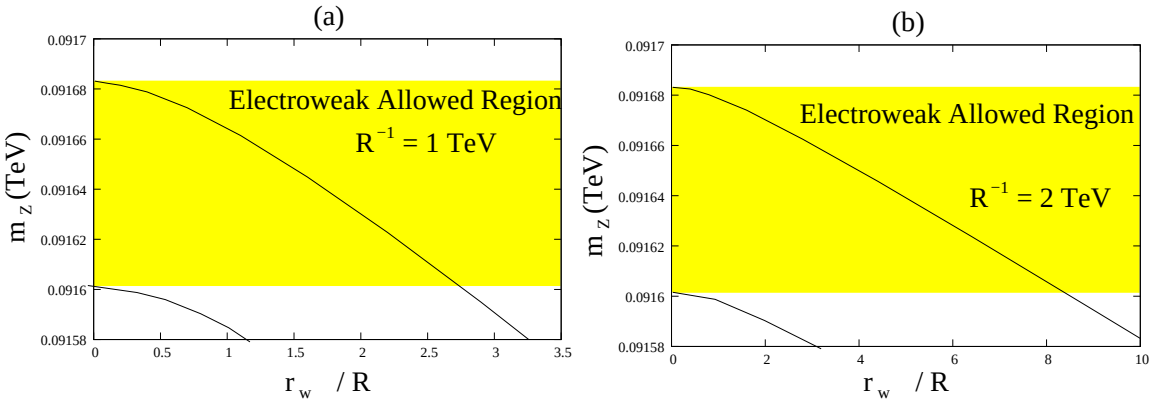

Figure 7: Variation of m_Z^{nUED} for different values of r_W with $R^{-1} = 1$ TeV and $R^{-1} = 2$ TeV in the $r_W \neq 0 = r_B = r_H$ scenario. The yellow (gray) band corresponds to the 2σ allowed tree-level value of m_Z^{tree}. The region within the black lines is the 2σ predicted tree-level value of m_Z^{nUED}.

to be

$$Q_{e_R} = \sum_{j=0}^{\infty} \int dy\, f_0^{e_R} U^T_{1(2j+1)} f_j^B f_0^{e_R} \tag{78}$$

$$Q_{e_L} = \frac{1}{2} \sum_{j=0}^{\infty} \left(\int dy\, f_0^{e_L} U^T_{1(2j+1)} f_j^B f_0^{e_L} + \int dy f_0^{e_L} U^T_{1(2j+2)} f_j^W f_0^{e_L} \right). \tag{79}$$

With the electric charge of the fermions determined, we calculate $\alpha = Q^2/4\pi$. We iterate this procedure with varying values of $\hat{g}_Y$ until the result matches the experimentally measured value $\alpha_{em} = 1/(127.925 \pm 0.016)$ to a precision of $(\alpha - \alpha_{em})/\alpha_{em} < 10^{-7}$ which lies an order of magnitude below the experimental error.[13] With the parameters $(\hat{g}_Y, \hat{g}_2, \hat{v})$ determined, we calculate the mass of the second lightest mass eigenstate which is identified with the tree level Z mass as defined in Eq. (54).

In Fig. 7 we show the value of m_Z^{nUED} for $R^{-1} = 1$ TeV and $R^{-1} = 2$ TeV, assuming a 2σ error in the input values of α, m_W and G_f. As in scenarios I and II we see that the bounds on r_W/R are weaker for increasing R^{-1}, and we again find that the bounds from tree level matching of the lowest lying modes to the Standard Model fields are weaker than the NDA estimate of $r_W/R \lesssim 6\pi/\Lambda R$. As for scenario II, we performed the analysis for the WWZ vertex modifications and we again find that it leads to weaker constraints than those from m_Z presented above.

[13] The equality of left-handed and right-handed couplings is guaranteed by 4D gauge invariance of the *full* model. In order to perform the diagonalization numerically, we truncate the mass matrix after the fourth KK level. The truncation leads to numerical values of $(\alpha_L - \alpha_R)/\alpha_L < 10^{-7}$ for the parameter regime of R, r_W considered in this article which is sufficiently low to not affect any of our results and justifies our truncation at the fourth KK level. As a consistency check, we verified numerically that $(\alpha - \alpha_{em})/\alpha_{em}$ decreases when truncating at a higher KK level. In our determination for $\hat{g}_Y$, we use Q_{e_L} to calculate α.

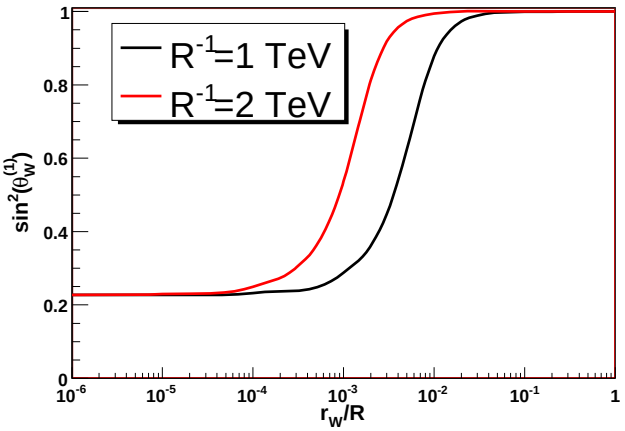

Figure 8: Modification of the Weinberg angle of the first KK mode as defined in Eq. (81) at $R^{(-1)} = 1$ TeV (black) and $R^{(-1)} = 2$ TeV (red/gray).

5.3.2 $W^{3(1)}$ dark matter

In the last section, we determined the 5 dimensional parameters $(\hat{g}_Y, \hat{g}_2, \hat{v})$ for a given set of parameters R, r_W and calculated the bound on r_W/R from matching the lowest lying KK modes to the standard model. With the parameter set $(r_W, R, \hat{g}_Y, \hat{g}_2, \hat{v})$, the full KK mass spectrum of the electroweak sector is determined and we can study the LKP.[14]

For $r_W \neq 0 = r_B = r_H$ it follows from Eq. (126)

$$\begin{aligned} m_{h^{(1)}} &> m_{a^{0(1)}} > m_{a^{\pm(1)}} > m_{W^{\pm(1)}} \\ m_{Z^{(1)}} &> m_{W^{\pm(1)}} \geq m_{A^{(1)}}, \end{aligned} \tag{80}$$

where $A^{(1)}$ and $Z^{(1)}$ denote the lightest and second lightest KK parity odd eigenvalue of the neutral gauge boson mass mixing matrix. In terms of the $B - W$ basis, they are defined in Eqs. (75) and (76) as $A^{(1)} = U^T_{3j}\mathcal{B}^j$ and $Z^{(1)} = U^T_{4j}\mathcal{B}^j$. As argued in the beginning of Section 5.3, the KK mode mixing contributions in this basis are suppressed and hence all $A^{(1)}$ components except $U^T_{33}B^{(1)}$ and $U^T_{34}W^{(1)}$ are sub-dominant. It is thus sensible to define the Weinberg angle at the first KK level by

$$\tan\theta_W^{(1)} \equiv U^T_{34}/U^T_{33}. \tag{81}$$

Fig. 8 shows the numerical result for $\sin^2(\theta_W^{(1)})$ as a function of r_W, calculated for $R^{-1} = 1$ and 2 TeV. As can be seen, for values of $r_W/R \sim \mathcal{O}(10^{-2})$ ($r_W/R \sim \mathcal{O}(10^{-3})$) for $R^{-1} = 1$ TeV ($R^{-1} = 2$ TeV), the LKP composition changes from a KK photon with Weinberg angle $\theta_W^{(1)} = \theta_{W,SM}$ to almost purely $W^{3(1)}$. The bounds on r_W/R derived in

[14] Again, in order to fully fix the Higgs boson KK spectrum, m_h and μ_b need to be specified, but assuming $m_h > 115$ GeV or $\mu_b > 0$ raises the Higgs KK masses without affecting the mass spectra of the electroweak gauge bosons or the charged and the pseudoscalar Higgs. The discussion of the LKP is therefore independent of m_h and μ_b.

the last section lie two or three orders of magnitude above these values, showing that $W^{3(1)}$ dark matter can easily be accomplished in the non-minimal UED models studied in this article.

As in scenario I and II, the first KK mode masses in this scenario are split. The fermion and gluon KK mode masses lie at the compactification scale R^{-1}. As we chose $r_H = 0$, the masses of the Higgs KK modes $h^{(1)}, a^{\pm,0(1)}$ lie at the compactification scale, too. Furthermore, the choice $r_B = 0$ leaves the mass of the heavier first KK level eigenstate of the neutral gauge boson mass matrix at the compactification scale. For $r_W/R \gtrsim 10^{-2}$, the LKP is almost purely $W^{3(1)}$. As is expected, only the masses of the $W^{\pm,3(1)}$ are reduced by the non-zero $SU(2)$ BLKT. As the mass splitting between $W^{\pm(1)}$ and $W^{3(1)}$ solely arises from the mixing in the neutral gauge boson sector, which is strongly suppressed for $r_W/R \gtrsim 10^{-2}$, the $W^{\pm(1)}$ and $W^{3(1)}$ masses are highly degenerate in our tree-level investigation.

We wish to emphasize that the analysis presented here is performed at tree-level, only. In the discussion of radiative corrections to MUED in Ref. [10], BLTs are assumed to vanish at the cutoff scale Λ. This assumption is used to justify neglecting the effect of KK-mode mixing on the mass spectrum and the modification of the KK-eigenfunctions. In this article we have shown that such modifications of the KK-eigenfunctions are a key aspect when considering non-vanishing BLTs. Therefore, a generalization of the results of Ref. [10] to the case of non-minimal UED is non-trivial. To give an estimate of the impact of radiative corrections, following Ref. [10], let us again consider the mass matrix of neutral gauge bosons at the first KK level in Eq. (62). Including radiative corrections, BLTs, and neglecting KK mode mixing, we can naively approximate the mass matrix to be

$$M^2_{B^{(1)},W^{3(1)}} = \begin{pmatrix} m^2_{B^{(1)}} + \hat{\delta}\left(m^2_{B^{(1)}}\right) & \mathcal{M}^2_{1,1} \\ \mathcal{M}^2_{1,1} & m^2_{W^{(1)}} + \hat{\delta}\left(m^2_{W^{3(1)}}\right) \end{pmatrix}, \tag{82}$$

where the matrix elements are defined as in Eq. (62) and $\hat{\delta}(m^2_{B^{(1)}})$ and $\hat{\delta}(m^2_{W^{3(1)}})$ are the radiative corrections to $m^2_{B^{(1)}}$ and $m^2_{W^{3(1)}}$ as given in Ref. [10]. In MUED, the radiative corrections drive the LKP to be almost purely $B^{(1)}$ because $m^2_{B^{(1)}} = 1/R^2 + m^2_B$, $m^2_{W^{3(1)}} = 1/R^2 + m^2_W$ and $\hat{\delta}(m^2_{B^{(1)}}) < 0 < \hat{\delta}(m^2_{W^{3(1)}})$. To arrive at a $W^{3(1)}$-like LKP, the BLT effects have to (over-)compensate the effect of radiative corrections. For $R^{-1} = 1$ TeV and $\Lambda R = 20$, the radiative corrections in Ref. [10] yield a splitting of ~ 60 GeV between the MUED $B^{(1)}$ and $W^{3(1)}$ masses which can compensated by a W BLKT with $r_W/R \gtrsim 0.1$. This value lies an order of magnitude below the NDA estimate $r_W/R \lesssim 6\pi/(\Lambda R) \approx 1$ and below the experimental constraints derived in this article. Therefore our simple approximation shows that a $W^{3(1)}$-like dark matter candidate is still conceivable, when taking radiative corrections into account.

6 Conclusions and Outlook

Models with a universal extra dimension should be considered as effective field theories with a cutoff at the PeV scale. Their symmetries allow for brane localized operators of

the same dimension as the standard UED bulk operators. Every brane localized term implies an unsuppressed free parameter. We argue that in a bottom-up approach to UED, all boundary localized operators should be included and their implications for phenomenology studied.

In this article, we extended earlier results on boundary localized operators [18, 20] in extra dimensional models and applied them to UED. We presented a framework to derive mass spectra and couplings for tree level UED with boundary localized kinetic and mass terms in the electroweak sector, including gauge fixing and identifying the Goldstone and physical Higgs KK modes. As we showed, the zero mode relations are generically modified when including BLTs. As the zero mode level of UED is identified with the Standard Model particles, modifications of the zero modes imply corrections to the Standard Model relations between masses and couplings *at the tree level*. In addition, BLTs affect the mass spectrum *and* couplings of the non-zero KK modes and thus have important implications for the collider phenomenology of UED KK modes as well as for the phenomenology of the UED dark matter candidate which is given by the lightest Kaluza Klein mode.

In order to demonstrate the phenomenological impact of boundary localized parameters in more detail, we presented three sample scenarios in which we derived constraints on the boundary parameters r_B, r_W, r_H which arise when matching the zero modes of the electroweak sector to the Standard Model. With the underlying parameters fixed by the matching we identified the lightest KK mode in the respective scenarios. In all sample scenarios studied, we showed that the inclusion of non-zero boundary kinetic terms change the 4D to 5D parameter matching, but once the correct relations are taken into account, the Standard Model relations are only weakly affected and lead to bounds on r_W, r_B and r_H which are substantially weaker than the NDA estimate of $r_B \sim r_W \sim r_H \sim 6\pi/(\Lambda R)$. On the contrary, non-zero boundary kinetic terms have a strong effect on the non-zero KK masses and couplings of the electroweak sector. We showed that masses of the electroweak KK partners equipped with a boundary localized kinetic term can lie substantially below the compactification scale while the first KK modes of the fermions and the gluon remain at a mass scale R^{-1}.[15]

Our first sample scenario, where we chose $r_W = r_B = r_H$, represents a very simple example of non-minimal UED with only four free parameters (R, r_{EW}, m_h, μ_b). In this scenario, the LKP is the KK photon for all allowed values of r_{EW}. For our second parameter choice, $r_B = r_W \equiv r_g \neq r_H$, we showed that the parameter space allowed by the electroweak constraints includes regions where the LKP is changed from a KK photon to either a KK charged Higgs $a^{\pm(1)}$ (which as a charged LKP is disfavored) or the KK Higgs $h^{(1)}$. The KK Higgs provides a new dark matter candidate in UED models. For a compactification scale of $R^{-1} = 1$ TeV, the $h^{(1)}$ LKP parameter space is strongly restricted, but it is opened up considerably for a compactification scale of $R^{-1} = 2$ TeV. In our final scenario with $r_W \neq r_B = 0 = r_H$, we showed that a $W^{3(1)}$-like LKP can

[15] With the content of this article, including a BLKT for the gluon is straight forward. This would reduce the KK gluon mass to the scales of the electroweak KK partners while still keeping the fermions heavy. This would realize a UED scenario which shares many qualitative features with split supersymmetry [25].

easily be achieved within the bounds on the zero mode spectrum studied in this article. $W^{3(1)}$-like dark matter presents another new UED dark matter candidate which is rarely considered in the literature, so far.[16] With the tools provided in this article (specifically in Appendix C), and the sample studies of Section 5, detailed studies of models with other non-minimal parameters (r_W, r_B, r_H, μ_b) are straight forward. Beyond providing calculational examples, Section 5 provides an instructive overview of the effects of BLTs on the electroweak sector of non-minimal UED at tree-level.

The work presented here is meant to be a small step towards a more complete mapping of the UED parameter space. We made the simplifying assumption that the boundary and bulk VEVs coincide which allowed us to expand around a flat VEV. For a general treatment, this assumption needs to be relaxed. We did not address boundary localized kinetic fermion terms in this article. All analysis presented in this article is at tree-level with BLTs only. On the contrary, the analysis of Ref.[10] is at one-loop level but ignoring non-zero BLTs at the cutoff scale. For a complete treatment of UED as an effective field theory a consistent description of UED with loop corrections in the presence of BLTs is needed in order to study constraints on the *full* UED parameter space along the lines of Refs. [5, 6, 8, 9]. In the light of upcoming LHC data and dark matter searches, a more complete mapping of the UED parameter space is needed in order to investigate the potential of UED to explain new signals and also to allow for an honest comparison of UED with other Standard Model extensions, *e.g.* along the lines of Refs.[15].

Acknowledgments

We thank Marcela Carena, Gordon Kane, Kyoungchul Kong, Mariano Quiros, Carlos Wagner, James Wells, and especially Aaron Pierce for helpful discussions. This work was supported by the MCTP and the DOE under grant DE-FG02-95ER40899.

Appendices

A Review and reformulation of electroweak symmetry breaking by a bulk Higgs on $S^1/\mathbb{Z}_2$

In this appendix we reformulate the gauge fixing procedure of Ref. [17] along the lines of Ref. [23]. This reformulation will enable us to generalize the gauge fixing procedure and the identification of the Goldstone modes and the physical Higgs modes to the electroweak sector of UED in the presence of boundary kinetic terms for the gauge and Higgs fields, which is presented in Appendix B.

[16] To our knowledge, the only more detailed investigation of $W^{3(1)}$-like dark matter and Higgs UED dark matter can be found in Ref. [14], which assumes couplings of the LKP that are not modified by non-trivial wavefunction overlap integrals.

A.1 The 5 dimensional abelian Higgs model

In order to present the method in the simplest setup first, consider the UED action of an abelian gauge field on $S^1/\mathbb{Z}_2$, spontaneously broken by a bulk Higgs field

$$S_{EW,bulk} = S_g + S_H \tag{83}$$

with

$$S_g = \int d^5x \left(-\frac{1}{4\hat{g}^2} A_{MN} A^{MN}\right) \tag{84}$$

$$S_H = \int d^5x \left((D_M H)^\dagger (D^M H) + \hat{\mu}^2 H^\dagger H - \hat{\lambda}(H^\dagger H)^2\right), \tag{85}$$

where the covariant derivative is $D_M = \partial_M - \frac{i}{2} A_M$. The 5 dimensional Higgs boson acquires an vacuum expectation value (VEV) $\hat{v} \equiv \sqrt{\hat{\mu}^2/\hat{\lambda}}$, and makes the 5 dimensional vector particle A_M massive. Now we can expand the 5 dimensional Higgs about the true vacuum

$$H = \frac{1}{\sqrt{2}} (v + h + i\chi) \tag{86}$$

where h is the physical scalar Higgs boson while χ is the pseudo-scalar Higgs component. To eliminate the bulk mixing term between the vector mode A_μ and the scalar modes A_5 and χ we can use the gauge fixing action

$$S_{GF} = \int \left(-\frac{1}{2\hat{g}^2 \xi_A} \left[\partial^\mu A_\mu - \xi_A \left(\partial_5 A_5 - \frac{\hat{g}^2 \hat{v}}{2} \chi\right)\right]^2\right), \tag{87}$$

which helps us identify the Goldstone mode as

$$G \equiv \partial_5 A_5 - \frac{\hat{g}^2 \hat{v}}{2} \chi. \tag{88}$$

Variation of the action yields the following equations of motion

$$\left[\Box - \partial_5^2 + 2\hat{\mu}^2\right] h = 0 \tag{89}$$

$$\left[\left(\Box - \partial_5^2 + \frac{\hat{g}^2 \hat{v}^2}{4}\right) \eta^{\mu\nu} - \left(1 - \frac{1}{\xi_A}\right) \partial^\mu \partial^\nu\right] A_\mu = 0 \tag{90}$$

$$-\frac{1}{\hat{g}^2} \left(\Box - \xi_A \partial_5^2 + \frac{\hat{g}^2 \hat{v}^2}{4}\right) A_5 + \frac{\hat{v}}{2} (1 - \xi_A) \partial_5 \chi = 0 \tag{91}$$

$$-(\Box - \partial_5^2 + \xi_A \frac{\hat{g}^2 \hat{v}^2}{4}) \chi - \frac{\hat{v}}{2} (1 - \xi_A) \partial_5 A_5 = 0. \tag{92}$$

Subtracting $\hat{g}^2$ times Eq. (91) from ∂_5 times Eq. (92) eliminates the ξ_A dependent part and allows us to identify the physical pseudo-scalar [17]

$$a \equiv -\partial_5 \chi + \frac{\hat{v}}{2} A_5, \tag{93}$$

whose equation of motion is given by

$$\left(\Box - \partial_5^2 + \frac{\hat{g}^2\hat{v}^2}{4}\right) a = 0 \tag{94}$$

In unitary gauge, $\xi_A \to \infty$, the Goldstone mode decouples and the resulting equations of motion of the remaining fields are

$$\left[\left(\Box - \partial_5^2 + \tfrac{\hat{g}^2\hat{v}^2}{4}\right)\eta^{\mu\nu} - \partial^\mu\partial^\nu\right] A_\mu = 0 \tag{95}$$

$$\left[\Box - \partial_5^2 + 2\hat{\mu}^2\right] h = 0 \tag{96}$$

$$G = 0 \tag{97}$$

The boundary conditions for the fields h, A_μ, and a are determined by demanding the variation of the boundary action to vanish. Before doing so, the remaining gauge freedom can be used to eliminate the boundary mixing term between A_μ and A_5 by adding the boundary gauge fixing term [23]

$$S_{GF,b} = \int d^4x(-\frac{1}{2\xi_{A,b}\hat{g}^2}\left(\partial_\mu A^\mu + \xi_{A,b}A_5\right)^2). \tag{98}$$

The variation of Eqs. (83), (87)and (98) in unitary gauge on the boundary yields

$$\begin{aligned}\delta S_{tot,b} &= \int d^4x \left(-\partial_5 h\delta h + \frac{1}{\hat{g}^2}\left[\frac{1}{\xi_{A,b}}\partial^\nu\partial_\mu A^\mu - \partial_5 A^\nu\right]\delta A_\nu\right. \\ &\left. + \frac{1}{\hat{g}^2}\left[-\xi_{A,b}A_5\right]\delta A_5 + a\delta\chi\right).\end{aligned} \tag{99}$$

Taking $\xi_{A,b} \to \infty$, and using the definitions of G and a in Eqs. (88,93), the boundary conditions following from Eq.(99) correctly reproduce the standard UED boundary conditions

$$\begin{aligned}\partial_5 A_\mu &= 0 \\ A_5 &= 0 \\ \partial_5 h &= 0 \\ \partial_5 \chi &= 0,\end{aligned} \tag{100}$$

which have been used in Ref. [17] as a starting point to derive the KK-decomposition of the UED model.

In the presence of additional boundary terms the bulk equations of motion Eqs. (95)-(97) are unchanged, but the boundary variations and therefore the boundary conditions on the KK wavefunctions are altered and affect the wavefunctions and mass spectra. We discuss the effects of boundary localized kinetic terms for gauge and the Higgs field in Appendix B.

A.2 Generalization to $SU(2) \times U(1)$

It is straightforward to generalize the results of the previous subsection to electroweak sector of UED. The only complicating factor is that the bulk action Eq. (1) contains mixing terms of the $U(1)$ and the electrically neutral $SU(2)$ gauge field $\propto \hat{v}^2 B^\mu W^3_\mu$ due to the Higgs transforming under both $U(1)_Y$ and $SU(2)_L$.

In the absence of any BLTs as discussed here, or if the boundary terms introduced induce the same mixing as the bulk terms, the mixing term can be removed by rotating into the 5 dimensional Z_μ, A_μ basis given by[17]

$$\begin{aligned} Z_M &= \frac{1}{\sqrt{\hat{g}_Y^2 + \hat{g}_2^2}} \left(W^3_M - B_M\right) \\ A_M &= \frac{1}{\sqrt{\hat{g}_Y^2 + \hat{g}_2^2}} \left(\frac{\hat{g}_Y}{\hat{g}_2} W^3_M + \frac{\hat{g}_2}{\hat{g}_Y} B_M\right). \end{aligned}$$

The bulk equations of motion in the Z_μ, A_μ basis are

$$\left[\left(\Box - \partial_5^2 + \tfrac{\hat{g}_2^2 \hat{v}^2}{4}\right)\eta^{\mu\nu} - \partial^\mu\partial^\nu\right] W^\pm_\mu = 0 \tag{101}$$

$$\left[\left(\Box - \partial_5^2 + \tfrac{(\hat{g}_Y^2+\hat{g}_2^2)\hat{v}^2}{4}\right)\eta^{\mu\nu} - \partial^\mu\partial^\nu\right] Z_\mu = 0 \tag{102}$$

$$\left[\left(\Box - \partial_5^2\right)\eta^{\mu\nu} - \partial^\mu\partial^\nu\right] A_\mu = 0 \tag{103}$$

$$\left[\Box - \partial_5^2 + 2\hat{\mu}^2\right] h = 0 \tag{104}$$

$$\left(\Box - \partial_5^2 + \tfrac{\hat{g}_2^2 \hat{v}^2}{4}\right) a^\pm = 0 \tag{105}$$

$$\left(\Box - \partial_5^2 + \tfrac{(\hat{g}_Y^2+\hat{g}_2^2)\hat{v}^2}{4}\right) a = 0 \tag{106}$$

$$G^\pm = G^3 = G_Y = 0, \tag{107}$$

where the fields $a, a^\pm, G^3, G^\pm, G_Y$ are defined by

$$\begin{aligned} a^\pm &= \partial_5 \chi^\pm + \frac{\hat{v}}{2} W^\pm_5 \\ a &= \partial_5 \chi^3 + \frac{\hat{v}}{2} Z_5 \\ G_{W^\pm} &= \partial_5 W^\pm_5 + \frac{\hat{g}_2^2 \hat{v}}{2} \chi^\pm \\ G_Z &= \partial_5 Z^3_5 + \frac{(\hat{g}_Y^2 + \hat{g}_2^2)\hat{v}}{2} \chi^3 \\ G_A &= \partial_5 A_5. \end{aligned} \tag{108}$$

The boundary conditions are determined from the variation of the boundary action. In the absence of any boundary terms other than terms arising from partial integrations

[17] Note that in this basis, the 5 dimensional kinetic terms of Z_M and A_M are canonically normalized, *i.e.* $S \supset -\frac{1}{4} A_{MN} A^{MN} - \frac{1}{4} Z_{MN} Z^{MN}$.

used to derive the bulk equations of motion, they read

$$\begin{aligned} \partial_5 W_\mu^\pm = 0 \qquad & W_5^\pm = 0 \\ \partial_5 Z_\mu = 0 \qquad & Z_5 = 0 \\ \partial_5 A_\mu = 0 \qquad & A_5 = 0 \\ \partial_5 h = 0 \qquad & \partial_5 \chi^3 = 0, \end{aligned} \tag{109}$$

as expected.

B UED with boundary localized terms

The reformulation of the gauge fixing procedure developed in the last section enables us to incorporate the BLTs of Eq.(24). The aim of this section is to derive the boundary conditions of all fields in the electroweak sector which we use Sec. 4 in order to calculate the wavefunctions and mass spectra. For illustration we again discuss the abelian model first and then outline the changes when generalizing to the full electroweak sector.

B.1 The abelian Higgs model in the presence of boundary terms

Expanding the abelian analog of the action in Eq. (24) around $\hat{v}$ to quadratic order yields the boundary terms

$$\begin{aligned} S_{BLKT,H} = \quad & \int d^5x \left[\delta(y) + \delta(y-\pi R)\right] \times \Big(\frac{r_H}{2} \partial_\mu h \partial^\mu h - \mu_b^2 h^2 \\ & + \frac{r_H}{2} \partial_\mu \chi \partial^\mu \chi - \frac{r_A}{4\hat{g}^2} A_{\mu\nu} A^{\mu\nu} - \frac{r_H \hat{v}}{2} \partial^\mu A_\mu \chi - \frac{r_H}{2} \left(\frac{\hat{v}}{2}\right)^2 A_\mu A^\mu \Big) . \end{aligned} \tag{110}$$

The brane localized mixing of the gauge field with χ can be eliminated by using a brane localized gauge fixing term

$$S_{GF,b} = -\frac{1}{2\xi_b \hat{g}^2} \int d^4x \left[\partial_\mu A^\mu + \xi_b \left(A_5 + \frac{r_H \hat{g}^2 \hat{v}}{2} \chi \right) \right]^2 . \tag{111}$$

The boundary variation from Eqs. (99, 110, 111) in the gauge $\xi_b \to \infty$ yields the boundary conditions

$$(\partial_5 + r_H \Box + 2\mu_b^2) h = 0 \tag{112}$$

$$\left(\partial_5 + r_A \left[\Box \eta_{\mu\nu} - \partial_\mu \partial_\nu \right] + r_H \left(\frac{\hat{g}\hat{v}}{2} \right)^2 \right) A^\nu = 0 \tag{113}$$

$$A_5 + \frac{r_H \hat{g}^2 \hat{v}}{2} \chi = 0 \tag{114}$$

$$-r_H \Box \chi - \partial_5 \chi + \frac{\hat{v}}{2} A_5 = 0. \tag{115}$$

The Higgs and gauge boundary conditions are decoupled, and can be used to derive the KK decomposition (see Sec. 4).

The boundary conditions for χ and A_5 mix. In the following we show how to identify the physical pseudo scalar mode a consistent with our bulk identifications Eqs. (88,93) and the boundary conditions from Eqs. (114,115). We start from the bulk equation of motion for a Eq. (106). As $G \equiv 0$ in unitary gauge, we know that

$$\partial_5 A_5 \equiv \frac{\hat{g}^2 \hat{v}}{2} \chi. \tag{116}$$

Using this equation, which holds for any y, we can manipulate Eq. (91) to get the bulk equation of motion for A_5[18]

$$\left(\Box - \partial_5^2 + \frac{\hat{g}^2 \hat{v}^2}{4} \right) A_5 = 0. \tag{117}$$

The boundary variation Eq. (115) together with Eq. (116) implies boundary conditions

$$(A_5 + \frac{r_H \hat{g}^2 \hat{v}}{2} \chi^3)|_{0,\pi \mathrm{R}} = 0 \tag{118}$$

$$\Rightarrow \left\{ \begin{array}{rcl} (A_5 + r_H \partial_5 A_5)|_{y=\pi R} & = & 0 \\ (A_5 - r_H \partial_5 A_5)|_{y=0} & = & 0. \end{array} \right. \tag{119}$$

The problem of finding the KK decomposition of A_5 is reduced to solving Eq. (117) with boundary conditions (119), which again resemble the structure discussed in Sec.3 and can be solved for in the same way. The solution for a is proportional to the solution determined and can be found from it by using Eqs. (93,116).The normalization condition for a follows by collecting the kinetic terms for A_5 and χ from the 5D action and using Eqn. (116)

$$\begin{aligned} S \subset & \int d^5x \frac{1}{2\hat{g}^2} \partial_\mu A_5 \partial^\mu A_5 + \frac{1}{2} \partial_\mu \chi \partial^\mu \chi [1 + r_H(\delta(y) + \delta(y - \pi R))] \\ = & \int d^5x \frac{1}{2\hat{g}^2} \partial_\mu A_5 \partial^\mu A_5 + \frac{1}{2\hat{g}^2} \frac{4}{\hat{g}^2 \hat{v}^2} \partial_\mu \partial_5 A_5 \partial^\mu \partial_5 A_5 [1 + r_H(\delta(y) + \delta(y - \pi R))] \end{aligned} \tag{120}$$

implying the normalization condition for a via

$$\delta_{ij} = \frac{1}{\hat{g}_I} \int dy \left\{ f_i^a f_j^a + \frac{1}{\hat{m}_a^2} f_i'^a f_j'^a \left(1 + r_H \left[\delta(y) + \delta(y - \pi R)\right]\right) \right\}, \tag{121}$$

where we defined $\hat{m}_a \equiv \hat{g}\hat{v}/2$.

[18]This solution is consistent with the boundary condition on χ in Eq (114): Imposing Eq. (118) on the boundary, Eq (114) reads

$$(\frac{2}{\hat{g}^2 \hat{v}} \Box A_5 - \partial_5 \chi + \frac{\hat{v}}{2} A_5)|_{0,\pi \mathrm{R}} = 0.$$

Using Eq (116) this becomes

$$\left(\Box - \partial_5^2 + \frac{\hat{g}^2 \hat{v}^2}{4} \right) A_5 = 0$$

i.e. the bulk equation of motion (117) which is satisfied everywhere.

B.2 Boundary terms and spontaneously broken $SU(2) \times U(1)$

The main difference compared to the abelian case again arises due to $B_\mu - W_\mu^3$ mixing. In Sec. A.2, we were able to diagonalize the bulk action because the kinetic terms had a global $U(1)$ symmetry involving the W_μ^3 and B_μ fields which was broken by the Higgs VEV. With the addition of the boundary terms, the global U(1) is broken, unless $r_B = r_W$, and hence the basis in which the kinetic terms are diagonal differs from that in which the bulk mass terms are diagonal.

If $r_B = r_W \equiv r_{EW}$, the generalization of the previous section is straightforward. Working in the Z_M, A_M basis defined in Eq. (32), the bulk equations of motion for all fields are given in Eqs. (101-107). The boundary terms in this basis read

$$\begin{aligned} S_{BLKT,B} \;= \int d^5x \;\; [\delta(y) + \delta(y-\pi R)] \Bigg(& -\frac{r_{EW}}{4} A_{\mu\nu} A^{\mu\nu} - \frac{r_{EW}}{4} Z_{\mu\nu} Z^{\mu\nu} - \frac{r_{EW}}{2\hat{g}_2^2} W^+_{\mu\nu} W^{-\mu\nu} \\ & r_H \Bigg(\frac{1}{2}\partial_\mu h \partial^\mu h + \frac{1}{2}\partial_\mu \chi^a \partial^\mu \chi^a - \frac{\hat{v}}{2}\partial^\mu W^\pm_\mu \chi^\mp + \left(\frac{\hat{v}}{2}\right)^2 W^+_\mu W^{-\mu} \\ & -\frac{1}{2}\frac{\sqrt{\hat{g}_Y^2 + \hat{g}_2^2}\hat{v}}{2} \partial^\mu Z_\mu \chi^3 + \left(\frac{(\hat{g}_Y^2 + \hat{g}_2^2)\hat{v}}{2}\right)^2 Z_\mu Z^\mu \Bigg) . \end{aligned} \tag{122}$$

The boundary conditions for $W_\mu^\pm$, Z_μ, and A_μ are all decoupled. For $W_\mu^\pm$ and Z_μ and the associated physical Higgs modes $a^\pm, a^0$, the discussion and results of the previous section apply with the simple replacements $r_A \to r_{EW}$ and $\hat{g} \to \hat{g}_2$ or respectively $\hat{g} \to \sqrt{\hat{g}_Y^2 + \hat{g}_2^2}$. Note, that again we find non-flat zero modes for the gauge bosons unless $r_{EW} = r_H$.

For the photon A_μ, no bulk and boundary mass terms are present. The zero mode of the photon is flat and massless, while the higher KK mode masses are reduced in the presence of the boundary kinetic term. Finally, the Higgs boundary conditions are unaltered as compared to the abelian case, so the expressions of the last section hold unmodified.

The general case $r_W \neq r_B$ is discussed in Sec 5.3.

C Summary of wavefunctions and mass spectra in the electroweak sector

For convenience, we summarize the mass spectra and wavefunctions for all fields in the electroweak sector in this appendix. For the neutral gauge sector, we give the expansions in the $A_\mu - Z_\mu$ basis which we use in the special case $r_W = r_B$, as well as in the $B_\mu - W_\mu^3$ basis. In the $B_\mu - W_\mu^3$, the $B_\mu - W_\mu^3$ mixing is treated as a mass insertion, *i.e.* after expanding in the $B_\mu - W_\mu^3$ KK basis given here, the off diagonal contributions from $B_\mu - W_\mu^3$ mixing has do be calculated *after* KK decomposing, and the resulting mass matrix has to be diagonalized as outlined in Sec. 5.3.

	m	m_b	r_Φ
W	$\hat{g}_2^2\hat{v}^2/4$	$r_H\hat{g}_2^2\hat{v}^2/4$	r_W
Z	$(\hat{g}_2^2+\hat{g}_Y^2)\hat{v}^2/4$	$r_H(\hat{g}_2^2+\hat{g}_Y^2)\hat{v}^2/4$	r_B
h	$\sqrt{2}\hat{\mu}$	$\sqrt{2}\mu_b$	r_H
$a_\pm$	$\hat{g}_2^2\hat{v}^2/4$	$r_H\hat{g}_2^2\hat{v}^2/4$	r_H
a_0	$(\hat{g}_2^2+\hat{g}_Y^2)\hat{v}^2/4$	$r_H(\hat{g}_2^2+\hat{g}_Y^2)\hat{v}^2/4$	r_H

Table 1: Substitutions needed to convert the results of the 5 dimensional massive scalar in Section 3 in those for the electroweak fields.

We give all equations in terms of the parameters $r_I, \hat{g}_I, m_I$ which are listed in Table 1 for the respective electroweak fields.

The general form of the wavefunctions is given by

$$f_\alpha^I = N_\alpha^I \begin{cases} \frac{\cosh\left(M_{I\alpha}\left(y-\frac{\pi R}{2}\right)\right)}{\cosh\left(\frac{M_{I\alpha}\pi R}{2}\right)} & \alpha \text{ even} \\ -\frac{\sinh\left(M_{I\alpha}\left(y-\frac{\pi R}{2}\right)\right)}{\sinh\left(\frac{M_{I\alpha}\pi R}{2}\right)} & \alpha \text{ odd} \end{cases} \tag{123}$$

$$f_n^I = N_n^I \begin{cases} \frac{\cos\left(M_{I(n)}\left(y-\frac{\pi R}{2}\right)\right)}{\cos\left(\frac{M_{I(n)}\pi R}{2}\right)} & n \text{ even} \\ -\frac{\sin\left(M_{I(n)}\left(y-\frac{\pi R}{2}\right)\right)}{\sin\left(\frac{M_{I(n)}\pi R}{2}\right)} & n \text{ odd} \end{cases}, \tag{124}$$

where

$$\begin{aligned} m_{I(\alpha)}^2 &= -M_{I(\alpha)}^2 + m_I^2 \\ m_{I(n)}^2 &= M_{I(n)}^2 + m_I^2, \end{aligned} \tag{125}$$

The mass determining equations are

$$\begin{aligned} b_\alpha^I &= \begin{cases} \tanh(\frac{\sqrt{m_I^2-m_{I(\alpha)}^2}\pi R}{2}) & \alpha \text{ even} \\ \coth(\frac{\sqrt{m_I^2-m_{I(\alpha)}^2}\pi R}{2}) & \alpha \text{ odd} \end{cases} \\ b_n^I &= \begin{cases} -\tan(\frac{\sqrt{m_{I(n)}^2-m_I^2}\pi R}{2}) & n \text{ even} \\ \cot(\frac{\sqrt{m_{I(n)}^2-m_I^2}\pi R}{2}) & n \text{ odd.} \end{cases} \end{aligned} \tag{126}$$

where $m_{I(i)}^2$ are the *physical* KK masses, and

$$b_i^h = \frac{r_H m_{h^{(i)}}^2 - 2\mu_b^2}{\sqrt{|m_{h^{(i)}}^2 - m_h^2|}} \quad b_i^G = \frac{r_G m_{G^{(i)}}^2 - r_H m_G^2}{\sqrt{|m_{G^{(i)}}^2 - m_G^2|}} \quad b_i^{a^{\pm,0}} = r_H\sqrt{|m_{a^{\pm,0(i)}}^2 - m_{a^{\pm,0}}^2|}. \tag{127}$$

where $i,j \in \{\alpha, n\}$ for the Higgs h, the additional Higgs degrees of freedom $a^{\pm,0}$, any gauge fields $G \in (W^{\pm,3}, B, Z, A)$.

The normalization conditions are

$$\delta_{ij} = \int dy f_i^h f_j^h \left(1 + r_H \left[\delta(y) + \delta(y - \pi R)\right]\right) \quad (128)$$

$$\delta_{ij} = \frac{1}{\hat{g}_I^2} \int dy f_i^{\tilde{G}} f_j^{\tilde{G}} \left(1 + r_{\tilde{G}} \left[\delta(y) + \delta(y - \pi R)\right]\right) \quad (129)$$

$$\delta_{ij} = \int dy f_i^{Z,A} f_j^{Z,A} \left(1 + r_{EW} \left[\delta(y) + \delta(y - \pi R)\right]\right) \quad (130)$$

$$\delta_{ij} = \frac{1}{\hat{g}_I^2} \int dy \left\{ f_i^{a^{\pm,0}} f_j^{a^{\pm,0}} + \frac{1}{\hat{m}^2_{a^{\pm,0}}} f_i'^{a^{\pm,0}} f_j'^{a^{\pm,0}} \left(1 + r_H \left[\delta(y) + \delta(y - \pi R)\right]\right) \right\}, \quad (131)$$

where $\tilde{G}$ denotes gauge fields $G \in (W^{\pm,3}, B)$. The difference in normalizations in the $W-B$ basis and the $Z-A$ basis of Eq. (32) arises because in the latter, the 5 dimensional kinetic terms are canonically normalized already, *i.e.* $S \supset -\frac{1}{4} A_{MN} A^{MN} - \frac{1}{4} Z_{MN} Z^{MN}$. The normalization conditions for $a^{\pm,0}$ follow as in Eq. (121).

References

[1] T. Appelquist, H. C. Cheng and B. A. Dobrescu, Phys. Rev. D **64** (2001) 035002 [arXiv:hep-ph/0012100].

[2] I. Antoniadis, Phys. Lett. B **246**, 377 (1990). I. Antoniadis, N. Arkani-Hamed, S. Dimopoulos and G. R. Dvali, Phys. Lett. B **436**, 257 (1998) [arXiv:hep-ph/9804398].

[3] R. Barbieri and A. Strumia, Phys. Lett. B **462** (1999) 144 [arXiv:hep-ph/9905281]. M. Papucci, arXiv:hep-ph/0408058. Z. Chacko, M. A. Luty and E. Ponton, JHEP **0007**, 036 (2000) [arXiv:hep-ph/9909248]. G. Bhattacharyya, A. Datta, S. K. Majee and A. Raychaudhuri, Nucl. Phys. B **760**, 117 (2007) [arXiv:hep-ph/0608208].

[4] R. S. Chivukula, D. A. Dicus and H. J. He, Phys. Lett. B **525**, 175 (2002) [arXiv:hep-ph/0111016].

[5] T. G. Rizzo, Phys. Rev. D **64** (2001) 095010 [arXiv:hep-ph/0106336]. C. Macesanu, C. D. McMullen and S. Nandi, Phys. Rev. D **66** (2002) 015009 [arXiv:hep-ph/0201300]. C. Macesanu, C. D. McMullen and S. Nandi, Phys. Lett. B **546**, 253 (2002) [arXiv:hep-ph/0207269]. J. A. R. Cembranos, J. L. Feng and L. E. Strigari, Phys. Rev. D **75**, 036004 (2007) [arXiv:hep-ph/0612157].

[6] T. Appelquist and H. U. Yee, Phys. Rev. D **67** (2003) 055002 [arXiv:hep-ph/0211023]. I. Gogoladze and C. Macesanu, Phys. Rev. D **74**, 093012 (2006) [arXiv:hep-ph/0605207].

[7] A. J. Buras, M. Spranger and A. Weiler, Nucl. Phys. B **660** (2003) 225 [arXiv:hep-ph/0212143].

[8] K. Agashe, N. G. Deshpande and G. H. Wu, Phys. Lett. B **514** (2001) 309 [arXiv:hep-ph/0105084]. A. J. Buras, A. Poschenrieder, M. Spranger and A. Weiler, Nucl. Phys. B **678** (2004) 455 [arXiv:hep-ph/0306158]. U. Haisch and A. Weiler, Phys. Rev. D **76**, 034014 (2007) [arXiv:hep-ph/0703064]. P. Colangelo, F. De Fazio, R. Ferrandes and T. N. Pham, Phys. Rev. D **73**, 115006 (2006) [arXiv:hep-ph/0604029]. P. Colangelo, F. De Fazio, R. Ferrandes and T. N. Pham, Phys. Rev. D **74**, 115006 (2006) [arXiv:hep-ph/0610044]. T. M. Aliev and M. Savci, Eur. Phys. J. C **50**, 91 (2007) [arXiv:hep-ph/0606225].

[9] T. Appelquist and B. A. Dobrescu, Phys. Lett. B **516**, 85 (2001) [arXiv:hep-ph/0106140]. K. Agashe, N. G. Deshpande and G. H. Wu, Phys. Lett. B **511**, 85 (2001) [arXiv:hep-ph/0103235]. F. J. Petriello, JHEP **0205** (2002) 003 [arXiv:hep-ph/0204067]. J. F. Oliver, J. Papavassiliou and A. Santamaria, Phys. Rev. D **67**, 056002 (2003) [arXiv:hep-ph/0212391].

[10] H. C. Cheng, K. T. Matchev and M. Schmaltz, Phys. Rev. D **66** (2002) 036005 [arXiv:hep-ph/0204342].

[11] G. Servant and T. M. P. Tait, New J. Phys. **4**, 99 (2002) [arXiv:hep-ph/0209262]; D. Majumdar, Phys. Rev. D **67**, 095010 (2003) [arXiv:hep-ph/0209277].

[12] G. Servant and T. M. P. Tait, Nucl. Phys. B **650** (2003) 391 [arXiv:hep-ph/0206071].

[13] H. C. Cheng, J. L. Feng and K. T. Matchev, Phys. Rev. Lett. **89**, 211301 (2002) [arXiv:hep-ph/0207125]. M. Kakizaki, S. Matsumoto, Y. Sato and M. Senami, arXiv:hep-ph/0508283; M. Kakizaki, S. Matsumoto, Y. Sato and M. Senami, Phys. Rev. D **71**, 123522 (2005) [arXiv:hep-ph/0502059]. F. Burnell and G. D. Kribs, arXiv:hep-ph/0509118. K. Kong and K. T. Matchev, arXiv:hep-ph/0509119. G. Bertone, G. Servant and G. Sigl, Phys. Rev. D **68**, 044008 (2003) [arXiv:hep-ph/0211342]; L. Bergstrom, T. Bringmann, M. Eriksson and M. Gustafsson, Phys. Rev. Lett. **94**, 131301 (2005) [arXiv:astro-ph/0410359]; L. Bergstrom, T. Bringmann, M. Eriksson and M. Gustafsson, JCAP **0504**, 004 (2005) [arXiv:hep-ph/0412001]. T. Bringmann, JCAP **0508**, 006 (2005) [arXiv:astro-ph/0506219]; E. A. Baltz and D. Hooper, JCAP **0507**, 001 (2005) [arXiv:hep-ph/0411053]. D. Hooper and G. D. Kribs, Phys. Rev. D **70**, 115004 (2004) [arXiv:hep-ph/0406026]. D. Hooper and G. D. Kribs, Phys. Rev. D **67**, 055003 (2003) [arXiv:hep-ph/0208261]. S. Matsumoto and M. Senami, Phys. Lett. B **633**, 671 (2006) [arXiv:hep-ph/0512003]. M. Kakizaki, S. Matsumoto and M. Senami, Phys. Rev. D **74**, 023504 (2006) [arXiv:hep-ph/0605280].

[14] S. Arrenberg, L. Baudis, K. Kong, K. T. Matchev and J. Yoo, arXiv:0805.4210 [hep-ph].

[15] H. C. Cheng, K. T. Matchev and M. Schmaltz, Phys. Rev. D **66** (2002) 056006 [arXiv:hep-ph/0205314];
A. J. Barr, Phys. Lett. B **596**, 205 (2004) [arXiv:hep-ph/0405052]. A. J. Barr, JHEP **0602**, 042 (2006) [arXiv:hep-ph/0511115]. M. Battaglia, A. Datta, A. De Roeck, K. Kong and K. T. Matchev, JHEP **0507**, 033 (2005) [arXiv:hep-ph/0502041];

J. M. Smillie and B. R. Webber, arXiv:hep-ph/0507170. A. Datta, K. Kong and K. T. Matchev, Phys. Rev. D **72**, 096006 (2005) [Erratum-ibid. D **72**, 119901 (2005)] [arXiv:hep-ph/0509246]. A. Datta, G. L. Kane and M. Toharia, arXiv:hep-ph/0510204. A. Alves, O. Eboli and T. Plehn, Phys. Rev. D **74**, 095010 (2006) [arXiv:hep-ph/0605067]. C. Csaki, J. Heinonen and M. Perelstein, JHEP **0710**, 107 (2007) [arXiv:0707.0014 [hep-ph]]. G. L. Kane, A. A. Petrov, J. Shao and L. T. Wang, arXiv:0805.1397 [hep-ph]. K. Hsieh and C. P. Yuan, Phys. Rev. D **78**, 053006 (2008) [arXiv:0806.2608 [hep-ph]]. M. Burns, K. Kong, K. T. Matchev and M. Park, arXiv:0808.2472 [hep-ph].

[16] D. Hooper and S. Profumo, Phys. Rept. **453**, 29 (2007) [arXiv:hep-ph/0701197].

[17] A. Muck, A. Pilaftsis and R. Ruckl, Phys. Rev. D **65**, 085037 (2002) [arXiv:hep-ph/0110391].

[18] G. R. Dvali, G. Gabadadze, M. Kolanovic and F. Nitti, Phys. Rev. D **64**, 084004 (2001) [arXiv:hep-ph/0102216].

[19] H. Georgi, A. K. Grant and G. Hailu, Phys. Lett. B **506**, 207 (2001) [arXiv:hep-ph/0012379].

[20] M. S. Carena, T. M. P. Tait and C. E. M. Wagner, Acta Phys. Polon. B **33** (2002) 2355 [arXiv:hep-ph/0207056].

[21] F. del Aguila, M. Perez-Victoria and J. Santiago, JHEP **0302**, 051 (2003) [arXiv:hep-th/0302023]. F. del Aguila, M. Perez-Victoria and J. Santiago, arXiv:hep-ph/0305119. F. del Aguila, M. Perez-Victoria and J. Santiago, Acta Phys. Polon. B **34**, 5511 (2003) [arXiv:hep-ph/0310353]. F. del Aguila, M. Perez-Victoria and J. Santiago, JHEP **0610**, 056 (2006) [arXiv:hep-ph/0601222].

[22] F. Coradeschi, S. De Curtis, D. Dominici and J. R. Pelaez, JHEP **0804**, 048 (2008) [arXiv:0712.0537 [hep-th]]. C. P. Burgess, C. de Rham and L. van Nierop, JHEP **0808**, 061 (2008) [arXiv:0802.4221 [hep-ph]].

[23] G. Cacciapaglia, C. Csaki, C. Grojean, M. Reece and J. Terning, Phys. Rev. D **72** (2005) 095018 [arXiv:hep-ph/0505001].

[24] C. Amsler *et al.* [Particle Data Group], Phys. Lett. B **667**, 1 (2008).

[25] N. Arkani-Hamed and S. Dimopoulos, JHEP **0506**, 073 (2005) [arXiv:hep-th/0405159]. G. F. Giudice and A. Romanino, Nucl. Phys. B **699**, 65 (2004) [Erratum-ibid. B **706**, 65 (2005)] [arXiv:hep-ph/0406088]. N. Arkani-Hamed, S. Dimopoulos, G. F. Giudice and A. Romanino, Nucl. Phys. B **709**, 3 (2005) [arXiv:hep-ph/0409232].